Ecological Complexity 42 (2020) 100826

Contents lists available at ScienceDirect

Ecological Complexity

journal homepage: www.elsevier.com/locate/ecocom

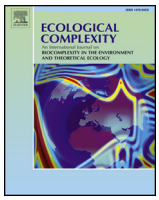

Impact of fear effect on the growth of prey in a predator-prey interaction model

Kankan Sarkar[a], Subhas Khajanchi[*,b]

[a] Department of Mathematics, Malda College, Malda, West Bengal 712101, India
[b] Department of Mathematics, Presidency University, 86/1 College Street, Kolkata 700073, India

ARTICLE INFO

Keywords:
Fear effect
Hopf bifurcation
Anti-predator defence
Stability analysis
Average Lyapunov functional

ABSTRACT

Several field data and experiments on a terrestrial vertebrates exhibited that the fear of predators would cause a substantial variability of prey demography. Fear for predator population enhances the survival probability of prey population, and it can greatly reduce the reproduction of prey population. Based on the experimental evidence, we proposed and analyzed a prey-predator system introducing the cost of fear into prey reproduction with Holling type-II functional response. We investigate all the biologically feasible equilibrium points, and their stability is analyzed in terms of the model parameters. Our mathematical analysis exhibits that for strong anti-predator responses can stabilize the prey-predator interactions by ignoring the existence of periodic behaviors. Our model system undergoes Hopf bifurcation by considering the birth rate r_0 as a bifurcation parameter. For larger prey birth rate, we investigate the transition to a stable coexisting equilibrium state, with oscillatory approach to this equilibrium state, indicating that the greatest characteristic eigenvalues are actually a pair of imaginary eigenvalues with real part negative, which is increasing for r_0. We obtained the conditions for the occurrence of Hopf bifurcation and conditions governing the direction of Hopf bifurcation, which imply that the prey birth rate will not only influence the occurrence of Hopf bifurcation but also alter the direction of Hopf bifurcation. We identify the parameter regions associated with the extinct equilibria, predator-free equilibria and coexisting equilibria with respect to prey birth rate, predator mortality rates. Fear can stabilize the predator-prey system at an interior steady state, where all the species can exists together, or it can create the oscillatory coexistence of all the populations. We performed some numerical simulations to investigate the relationship between the effects of fear and other biologically related parameters (including growth/decay rate of prey/predator), which exhibit the impact that fear can have in prey-predator system. Our numerical illustrations also demonstrate that the prey become less sensitive to perceive the risk of predation with increasing prey growth rate or increasing predators decay rate.

1. Introduction

Predator-prey interplay is a crucial topic in theoretical ecology and evolutionary biology which has been investigated by many scientists over the last few decades, and mathematical models have played a key role to better understand these complex scenarios. Representing the dynamics of predator-prey interactions through mathematical models seems to have been developed by Malthus in early nineteenth century. The mathematical model was eventually improved by incorporating linear per-capita birth rate of the prey species that resulted in the famous logistic growth model. The well-known Lotka-Volterra model was subsequently improved by adding logistic growth term for the prey and variety of population dependent response functions have been established which empowered realistic representation of the interplays among predator and prey population (Holling, 1959a; 1965; Ruan and Xiao, 2001). Similarly, the birth rate of prey population has also been subjected to improvements through introduction of fear effects (Hua et al., 2014; Wang et al., 2016; Wang and Zou, 2017; Zanette et al., 2011). The effect of fear has played a key role in theoretical ecology and environmental biology.

In presence of predator population the prey population may significantly change their behavior, such an scope that it could influence the prey population more effective than direct predation (Creel and Christianson, 2008; Hua et al., 2014; Lima and Dill, 1990). Most of the investigations on predator-prey interactions, only consider the direct assassination of prey population in presence of predators, as this predation is more easy to investigate in ecological systems and hence we focus on an effect of fear. Some ecologists and evolutionary biologists

* Corresponding author.

https://doi.org/10.1016/j.ecocom.2020.100826
Received 25 September 2019; Received in revised form 19 December 2019; Accepted 29 February 2020
Available online 12 March 2020
1476-945X/

have perceived the following fact based on field observations: a predator-prey system should include not only the direct killing factor but also the cost for fear (Cresswell, 2011; Hua et al., 2014; Lima and Dill, 1990; Zanette et al., 2011) but in lack of direct experimental observations, this fear effect has not been studied in the mathematical models. They noticed an attractive scenario that in presence of fear for predator population may influence the behavior and psychology for prey species more powerfully than direct assassination. The indirect effects caused by anti-predator behaviors (which incorporates foraging, habitat alterations, vigilance and various physiological alterations) for prey population may play a crucial role in governing prey demography (Preisser and Bolnick, 2008). The fear of predator population may influence the physiological situation for the prey species and it may cause a long-term loss for prey species. As for example, in the Greater Yellowstone Ecosystem, wolves (Canis lupus) influence the reproductive physiology of elks (*Cervus elaphus*) (Creel et al., 2007). Also, the frightened prey species naturally forages less, for which their growth rate decreases and embraces some survival mechanisms like starvation (Creel and Christianson, 2008; Cresswell, 2011). Higher level of acute risk for predation can create prey species to quit habitats or foraging sites momentarily, returning only when the acute risk has passed and the prey species are relatively safe (Cresswell, 2011). As for example, birds react to the sound of predator species with anti-predator defenses and they escape from their eyries at the first indication of danger. Such anti-predator activities may reduce the reproduction rate of the birds as a long-run cost, although it is temporarily lucrative as it increases the survival probability of mature birds (Cresswell, 2011).

In the year 2011, Zanette et al. (2011) studied a field experiment on song sparrows (*Melospiza melodia*) during a whole breeding season and observed that there is 40% depletion in offspring reproduction of song sparrows due to fear for predators (Zanette et al., 2011). This depletion is being happen due to the anti-predator activities which influences on growth rate, as well as the offspring survival rates because female song sparrows laid few eggs. Some of those eggs survived while most of the nestlings perished in the nest. The authors also observed that there were a variety of anti-predator responses of this effect. As for illustrations, frightened parents suckled their nestlings less, their nestlings were lighter and much more likely to perish. Correlational affirmation for birds (Eggers et al., 2006; Fontaine and Martin, 2006; Ghalambor et al., 2013; Hua et al., 2014), Elk (Creel et al., 2007), Snowshoe hares (Sheriff et al., 2009) and dugongs (Wirsing and Ripple, 2011) also give some confirmation that fear can influence the predator-prey interplays. Very recently, (Elliott et al., 2017), conducted a field observation on *Drasophila melanogaster* as prey species and *mantid* as their predators, to quantify the affect of fear for fitness of the populations in relation to species density. The authors showed that in appearance of *mantid*, the reproductive achievement of drasophila decreases, at low species density, in both their breeding as well as non-breeding seasons.

Predator-prey interactions with behavior for both prey and predator population utilizing the diversity of functional responses, have been observed substantially in the existing literatures. Most of literatures focused on the direct assassination of prey population by predator population, no matter how they are complicated interactions. To date, very few models have introduced the anti-predator activities for prey population in addition to the behavior for predators (Das and Samanta, 2018; Wang et al., 2016; Wang and Zou, 2017; Zhanga et al., 2019). Depends on the experimental work by Wang et al. (2016); Zanette et al. (2011) develop a mathematical model for predator-prey system by introducing cost of fear for prey species due to predators, where the cost of fear plays a vital role in the birth rate of prey. The authors showed that the strong anti-predator activities or correspondingly the major cost of fear may eliminate the existence of periodic behaviors and thus exclude the scenarios “paradox of enrichment”. They also showed that the fear can stabilize the system by eliminating population oscillations as observed in the predator-prey interactions. Additionally, under comparatively low cost for fear, periodic oscillations may persist, which emerging from either supercritical or subcritical Hopf bifurcation (Wang et al., 2016). Thus, fear effect can produce multi-stability in the predator-prey interactions. Wang and Zou (2017), formulate a stage-structured predator-prey interplays with adaptive avoidance for predator populations by incorporating the effect of fear of predator population for prey population. They divide the prey species into juvenile and mature stage and is obviously constituted by a system of delay differential system with maturation delay. They analyze their model dynamics with either a constant defense level or an adaptive defense level, respectively. Das and Samanta (2018) studied a stochastic predator-prey model with fear effect due to predator populations on prey populations when the predator is provided additional food.

In population dynamics of predator-prey interactions with variety of functional responses have been investigated by many scientists and the existence of limit cycle for predator-prey system has been established (Khajanchi, 2017a; Kuang and Freedman, 1988; Sugie et al., 1997). There have been many other prey-predator interactions that have modeled with more complicated response functions. As for illustrations, within the prey dependent response functions (Holling, 1959a; 1965; May, 1972), studied some monotone functional responses (Ruan and Xiao, 2001) and investigated some non-monotone response functional responses (Freedman and Wolkowicz, 1986). Additionally, these type of response functions depends on prey densities only, there are also studies introducing response functions depends on both the prey and predator densities, among which are the Cowley-Martin response function, Beddington-DeAngelis response function, Monod-Haldane response function (Beddington, 1975; Chinnathambi and Rihan, 2018; De Angelis et al., 1975; Khajanchi, 2014; 2017a; Ryu et al., 2018)and ratio dependent response function (Khajanchi and Banerjee, 2017; Kuang and Freedman, 1988; Ruan and Xiao, 2001). Takeuchi et al. (2009) investigated the dissension among investing time on taking care for immature and searching for food/nutrients of mature prey in absence of straight predation, whilst they presumed that the matures adapt their parental care time via learning. Krivan (2007) observed that the trade-off among foraging and predation based on typical Lotka-Volterra predator-prey system where either prey species or predator species or both were adaptive to maximize their independent robustness.

Influenced by the above literatures and the experimental observation of Zanette et al. (2011) for song sparrows (*Melospiza melodia*), and as an inclusion of Wang et al. (2016), in this manuscript, we propose and analyze a predator-prey system introducing the cost of fear to influence the indirect impact of predators on the prey population. The organization of this present paper is as follows. In the next section, we introduced the mathematical model for predator-prey system introducing the cost of fear generated by anti-predator activities and discuss the well-posedness of the system. In the same section, we explore the basic dynamical properties of the model including the positivity of the model, boundedness of the solutions and permanence of the system. Section 3 is dedicated to the analysis of local stability for the biologically feasible equilibrium points, existence and uniqueness of limit cycle. We also study the conditions for the occurrence of the Hopf bifurcation around the coexistence equilibrium point along with its direction and stability. Our model analysis represents that while introducing the effect of fear (predation risk) into the prey-predator interactions do not affect the mechanism of equilibrium points, it may alter the stability of equilibrium points. In the Section 4, we added analytical findings by numerical simulations which shows some potential roles that the fear effect may play in the dynamics of predator-prey interplays. The paper concludes in Section 5, in which we briefly summarize the biological indications of our analytical findings and possible future scope related to this paper.

2. The model

Let $N(t)$ and $P(t)$ be the densities of prey and predator populations at any time $t > 0$, respectively. We consider a predator-prey model and the cost of fear. We consider that the prey population follow a logistic growth without any predator population. The logistic growth for prey species can be divided into three parts, namely the birth rate of prey r_0, natural death rate and a density dependent decay rate due to the intra-species competition. Thus, the prey population can be modeled as follows

$$\frac{dN}{dt} = r_0 N - \delta_1 N - \gamma N^2, \tag{1}$$

where δ_1 represents the death rate for prey population, γ represents the decay rate of prey due to intra-species competition.

Several field data and experimental observations demonstrate that the fear effect reduces the production of prey species, we thus modify the model (1) by multiplying the production term by a function $f(\alpha, \eta, P)$ that accounts for the cost of anti-predator dependence due to fear, and the system (1) becomes

$$\frac{dN}{dt} = r_0 N f(\alpha, \eta, P) - \delta_1 N - \gamma N^2, \tag{2}$$

where the parameter α stands the level of fear which implies the anti-predator dependent scenarios for the prey population and η represents the cost of minimum fear. Now, we introduce a predation term $g(N)P$ into the model (2), to get the following predator-prey system with fear effect, leads to

$$\begin{aligned} \frac{dN}{dt} &= r_0 N f(\alpha, \eta, P) - \delta_1 N - \gamma N^2 - g(N)P, \\ \frac{dP}{dt} &= P(-\delta_2 + \theta g(N)), \end{aligned} \tag{3}$$

where δ_2 represents the death rate of predator populations, θ is the conversion coefficient for prey biomass to the predators and $g(N)$ is the functional response of the predator to prey density which means prey consumed per predator per unit time.

2.1. Functional response

The intake rate for predators as a function of prey density is called functional response in ecology. Here we have considered widely used Holling type II response function (Holling, 1959b), and for the mean time, for simplicity of model analysis, we adopt the following particular form:

$$g(N) = \frac{\beta N}{1 + \xi N}, \tag{4}$$

where parameters β and ξ are nonnegative constants.

2.2. Fear function

In our study, we consider the following fear function to measure the cost of fear

$$f(\alpha, \eta, P) = \eta + \frac{\alpha(1-\eta)}{\alpha + P}, \tag{5}$$

where α represents the level of fear and $\eta \in [0, 1]$ indicates the minimum cost of fear. The units of all the parameters are presented in the Table 1. Due to biological significance of α, P and $f(\alpha, \eta, P)$, it is worthy to assume that $f(0, \eta, P) = \eta$, $f(\alpha, \eta, 0) = 1$, $\lim_{P\to\infty} f(\alpha, \eta, P) = \eta$ but $\lim_{\alpha\to\infty} f(\alpha, \eta, P) = 1$. Here, $f(0, \eta, P) = \eta$ means that the prey population always remains under minimum fear η and $f(\alpha, \eta, 0) = 1$ means that in absence of predator the fear function has no effect in the growth of prey population. $\lim_{P\to\infty} f(\alpha, \eta, P) = \eta$ means that even if predator population increases infinitely large, the prey population will stress under minimum fear due to physiological impact when the prey populations are habituated with fear from predator species. $\lim_{\alpha\to\infty} f(\alpha, \eta, P) = 1$ indicates that after certain level of fear with prey population the fear function has no effect due to physiological impact when they are habituated.

Table 1
The description of the model parameters and variables and their units/dimensions.

Symbol	Description	Units/Dimension
N	Density of prey population	Mass
P	Density of predator population	Mass
r_0	Birth rate of prey population	1/Time
δ_1	Natural death rate of prey	1/Time
γ	Decay rate due to intraspecies competition	1/Mass.1/Time
β	Rate of predation	1/Mass.1/Time
ξ	Handling time	1/Mass
θ	Conversion rate of prey biomass to predator biomass	Dimensionless
δ_2	Death rate of predator	1/Time
η	Cost of minimum fear	Dimensionless
α	Level of fear	Mass

Previous studies (Wang et al., 2019; 2016) have considered $\lim_{\alpha\to\infty} f(\alpha, \eta, P) = 0$, but in our study we obtained $\lim_{\alpha\to\infty} f(\alpha, \eta, P) = 1$. Zanette et al. (2011) experimentally observed the effect of fear on offspring songbirds and found that offspring songbirds reduces 40% reproduction per year due to the effect of fear. This experiment shows that prey population have not stopped the reproduction due to fear. Mondal et al. (2018) has shown theoretically that prey population shows stable behavior from chaotic behavior as the level of fear increases. This result is biologically meaningful, because the prey population is aware and show signs of habituation after certain level of fear. That is after certain level, fear has no effect on prey population as prey population is aware and show sign of habituation and therefore in our model we have consider $\lim_{\alpha\to\infty} f(\alpha, \eta, P) = 1$. Fig. 1 shows the graphical representation of fear function. As the number of predator increases the value of fear function decreases though the prey population remains under minimum level of fear η. Since the fear factor multiplies with prey growth rate in the model, so the growth of prey population will be low when the value of fear function is low, that is, when predator population is high. Incorporating the cost of fear for prey species due to predator species, the model depicting the

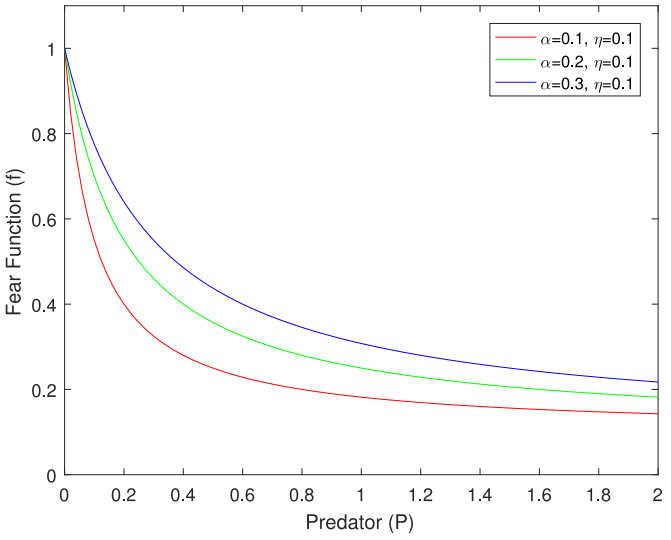

Fig. 1. The figure shows that the value of fear function decreases as the level of fear increases. The fear function has been plotted for different value of α as explained in the inset.

interaction between predator-prey population is given by the following system of nonlinear ordinary differential equations:

$$\begin{aligned}\frac{dN}{dt} &= r_0 N\left[\eta + \frac{\alpha(1-\eta)}{\alpha + P}\right] - \delta_1 N - \gamma N^2 - \frac{\beta NP}{1+\xi N},\\ \frac{dP}{dt} &= \frac{\theta\beta NP}{1+\xi N} - \delta_2 P.\end{aligned} \tag{6}$$

The model system (6) is subjected to the positive initial values $N(0) = N_0 \geq 0$, $P(0) = P_0 \geq 0$ of the population model.

The right hand side for the system (6) is a continuous functions of dependent variables, after integration of the first equation of (6), we have

$$N(t) = N(0)\exp\left(\int_0^t \left[r_0\left\{\eta + \frac{\alpha(1-\eta)}{\alpha + P(s)}\right\} - \delta_1 - \gamma N(s) - \frac{\beta P(s)}{1+\xi N(s)}\right]ds\right).$$

Similarly, from the second equation of (6), we have

$$P(t) = P(0)\exp\left(\int_0^t \left[\frac{\theta\beta N(s)}{1+\xi N(s)} - \delta_2\right]ds\right).$$

From the above expressions it is clear that $N(t)$ and $P(t)$ remain non-negative for infinite time if they initiate in the interior point of

$$\mathbf{R}_+^2 = \{(N(t), P(t)): N(t) \geq 0, P(t) \geq 0\}.$$

Hence $\mathbf{R}_+^2$ is positively invariant for the predator-prey model (6).

Lemma 2.1. *All the solutions of (6) with non-negative initial conditions (N_0, P_0), which initiate in R_+^2 are uniformly bounded.*

Proof. The proof of this Lemma is given in Appendix A. □

Note: From the ecological view point, the boundedness of the model (6) indicates that the interacting species are biologically well-behaved. Boundedness of the solutions implies that none of the interacting populations grow abruptly or exponentially for a long period of time. The number of each of the populations is bounded due to limited resource or source of food/nutrient.

2.3. Permanence of the system

The permanence of the model system plays a key role in ecology or evolutionary biology since the conditions of permanence for ecological models is a state guarantees the long-term survival of all the interacting species. From the mathematical view point its mean that the solutions of the system under consideration are away from zero. Here, we prove the permanence result directly by using average Lyapunov functional (Gard and Hallam, 1979; Khajanchi, 2017b), as our system (6) is uniformly bounded.

Theorem 2.1. *The system (6) is permanent if $r_0 > r_0^{[c]}$ with $\theta > \frac{\delta_2\xi}{\beta}$.*

Proof. To prove the theorem, we consider the average Lyapunov functional for the system (6) is

$$\mathcal{L}(N, P) = N^{\rho_1}P^{\rho_2},$$

where ρ_1 and ρ_2 are nonnegative constants. In the interior of the positive quadrant, we have

$$\begin{aligned}\triangle(N, P) = \frac{\dot{\mathcal{L}}(N,P)}{\mathcal{L}(N,P)} &= \rho_1\frac{\dot{N}}{N} + \rho_2\frac{\dot{P}}{P}\\ &= \rho_1\left[r_0\left\{\eta + \frac{\alpha(1-\eta)}{\alpha+P}\right\} - \delta_1 - \gamma N - \frac{\beta P}{1+\xi N}\right] + \rho_2\left[\frac{\theta\beta N}{1+\xi N} - \delta_2\right].\end{aligned}$$

Now, in order to investigate the permanence of the solution for the model (6), we must have to verify that $\triangle(N, P) > 0$ at the axial equilibrium point E_1. After some algebraic manipulations, we obtain that the condition $\triangle(N, P) > 0$ holds if $r_0 > r_0^{[c]}$, where $r_0^{[c]} = \delta_1 + \frac{\delta_2\gamma}{\theta\beta - \delta_2\xi}$ with $\theta > \frac{\delta_2\xi}{\beta}$, that is, the birth rate for prey population is higher than a threshold value and the conversion rate of predator population is higher than the ratio of natural decay rate for predator species and the search rate for predator population. This completes the Theorem. □

Note: In absence of the fear effect for prey species due to predator population does not influence the permanence of the model system under consideration.

3. Equilibria and their stability

3.1. Existence of steady states

Biologically feasible singular points are the points of intersection of the zero growth isoclines $r_0N\left[\eta + \frac{\alpha(1-\eta)}{\alpha+P}\right] - \delta_1 N - \gamma N^2 - \frac{\beta NP}{1+\xi N} = 0$ and $\frac{\theta\beta NP}{1+\xi N} - \delta_2 P = 0$, in the non-negative quadrant $\mathbf{R}_+^2 = \{(N(t), P(t)): N(t) \geq 0, P(t) \geq 0\}$. The prey nullcline is the straight line that is parallel to predator(P)-axis and the equation of the prey nullcline is $N = \frac{\delta_2}{\theta\beta - \xi\delta_2}$ and also it lies in the first quadrant with parameter restriction $\theta > \frac{\delta_2\xi}{\beta}$. Irrespective of the system parameters for the model (6) possesses three biologically meaningful singular points in $\mathbf{R}_+^2$, namely

(i) trivial singular point $E_0(0, 0)$, (ii) axial singular point $E_1(\bar{N}, 0)$, where $\bar{N} = \frac{r_0 - \delta_1}{\gamma}$, which is feasible if $r_0 > \delta_1$, that is, the birth rate of prey is higher than the natural death rate of prey population. Otherwise, E_1 become the extinct equilibrium point E_0, and (iii) the coexisting singular point $E^*(N^*, P^*)$, where

$$N^* = \frac{\delta_2}{\theta\beta - \xi\delta_2},$$

and P^* is the nonnegative root(s) of the quadratic equation

$$\sigma_1 P^{*2} + \sigma_2 P^* + \sigma_3 = 0, \tag{7}$$

where

$$\begin{aligned}\sigma_1 &= \beta,\\ \sigma_2 &= \alpha\beta + \gamma\xi N^{*2} + \delta_1\xi N^* + \gamma N^* + \delta_1 - r_0\eta - r_0\xi\eta N^*,\\ \sigma_3 &= \alpha\gamma\xi N^{*2} + \alpha\delta_1\xi N^* + \alpha\gamma N^* + \alpha\delta_1 - r_0\alpha - r_0\alpha\xi N^*.\end{aligned}$$

Now, for the existence of P^*, we consider the following two cases:

Case I: If $\sigma_3 < 0$, then the quadratic Eq. (7) has a unique non-negative root given by

$$P^* = \frac{-\sigma_2 + \sqrt{\sigma_2^2 - 4\sigma_1\sigma_3}}{2\sigma_1}.$$

For $\sigma_3 < 0$ gives the simplified form as $r_0 > \delta_1 + \gamma N^*$, with $N^* = \delta_2/(\theta\beta - \xi\delta_2)$. For $\theta > \xi\delta_2/\beta$ gives the positiveness of N^*. Explicit expression for a unique root of P^* is given by

$$P^* = \frac{-l_1 + \sqrt{\alpha^2\beta^2 + l_2 + (1+\xi N^*)^2(\delta_1 + \gamma N^* - r_0\eta)^2}}{2\beta}, \tag{8}$$

where $l_1 = \alpha\beta + (1+\xi N^*)(\delta_1 + \gamma N^* - r_0\eta)$ and $l_2 = 2\alpha\beta(1+\xi N^*)[2r_0 - (\delta_1 + \gamma N^* + r_0\eta)]$. Numerical results of mutual position of the prey and predator zero growth isoclines are plotted in the Fig. 2(a) and (b) for unique positive root with prey growth rate $r_0 = 0.7$ and 0.8 respectively. In the Fig. 2((a), (b)), the black dotted line represents the prey isocline and the corresponding solid blue line represents the predator isocline for $r_0 > \delta_1 + \gamma N^*$ and $\theta > \xi\delta_2/\beta$.

Case II: If $\sigma_2 < 0$ and $\sigma_3 > 0$, then the quadratic Eq. (7) will have two nonnegative roots are given by (provided $\sigma_2^2 > 4\sigma_1\sigma_3$)

$$P^* = \frac{-\sigma_2 \pm \sqrt{\sigma_2^2 - 4\sigma_1\sigma_3}}{2\sigma_1}.$$

For $\sigma_3 > 0$ gives the simplified version as $r_0 < \delta_1 + \gamma N^*$, where $N^* = \delta_2/(\theta\beta - \xi\delta_2)$. For $\theta > \xi\delta_2/\beta$ gives the positiveness of N^*. For $\sigma_2 < 0$ gives $\frac{1}{\eta}\left[(\delta_1 + \gamma N^*) + \frac{\alpha\delta_2}{\theta N^*}\right] < r_0$. Combining the cases for $\sigma_3 > 0$ and $\sigma_2 < 0$, we obtain $\frac{1}{\eta}\left[(\delta_1 + \gamma N^*) + \frac{\alpha\delta_2}{\theta N^*}\right] < r_0 < \delta_1 + \gamma N^*$.

Numerical simulations of mutual positions of the prey and predator zero growth isoclines are plotted in the Fig. 2(c), for two positive roots with prey growth rate $r_0 = 0.9$. In the Fig. 2(c), the black dotted line represents the prey isocline and the corresponding solid blue line represents the predator isocline for $\frac{1}{\eta}\left[(\delta_1 + \gamma N^*) + \frac{\alpha\delta_2}{\theta N^*}\right] < r_0 < \delta_1 + \gamma N^*$ and $\theta > \xi\delta_2/\beta$. The Fig. 2(d) represents that there is no mutual position for the prey and predator zero growth isocline with prey growth rate $r_0 = 1.4$. For the Case I and Case II, the model system (6) will have positive interior equilibrium point.

3.2. Local stability analysis

In this subsection, we shall study the local asymptotic stability of the biologically feasible singular points and Hopf bifurcation criterion of the coexisting singular point $E^*(N^*, P^*)$ for the system (6). To investigate the local asymptotic stability, we compute the variational matrix for the model system (6) at any point (N, P) is given by

$$J_E = \begin{bmatrix} F_N & F_P \\ G_N & G_P \end{bmatrix},$$

where

$$F_N = r_0\left[\eta + \frac{\alpha(1-\eta)}{\alpha + P}\right] - \delta_1 - 2\gamma N - \frac{\beta P}{1+\xi N} + \frac{\beta\xi NP}{(1+\xi N)^2};$$

$$G_P = \frac{\theta\beta N}{1+\xi N} - \delta_2,$$

$$F_P = -\frac{\alpha(1-\eta)r_0 N}{(\alpha+P)^2} - \frac{\beta N}{1+\xi N}; \quad G_N = \frac{\theta\beta P}{1+\xi N} - \frac{\theta\beta\xi NP}{(1+\xi N)^2}.$$

At the critical point $E_0(0, 0)$, the eigenvalues of the variational matrix J_{E_0} of (6) are given by $r_0 - \delta_1$ and $-\delta_2$. The trivial singular point E_0 is locally asymptotically stable if $r_0 < \delta_1$. That is, the death rate of prey is larger than the growth rate of prey. Thus, if the trivial equilibrium point E_0 is stable asymptotically, then the boundary singular point E_1 does not exist. Also in reality, the death rate of prey can not be higher than the growth rate of prey. The results can be stated in the following theorem.

Theorem 3.1. *The trivial singular point $E_0(0, 0)$ is always unstable.*

Evaluating the Jacobian matrix for the system (6) at the boundary singular point $E_1(\frac{r_0-\delta_1}{\gamma}, 0)$, we obtain the eigenvalues are $\lambda_1 = -\gamma\bar{N} = \delta_1 - r_0$ and $\lambda_2 = \frac{\theta\beta\bar{N}}{1+\xi\bar{N}} - \delta_2 = \frac{\theta\beta(r_0-\delta_1)}{\gamma+\xi(r_0-\delta_1)} - \delta_2$. The boundary singular point E_1 will be locally asymptotically stable if $\lambda_1 < 0$ and $\lambda_2 < 0$, that is, $r_0 > \delta_1$ and $r_0 < \delta_1 + \frac{\delta_2\gamma}{\theta\beta - \delta_2\xi}$ respectively. Biologically, $r_0 > \delta_1$ implies that the birth rate of prey population is higher than the death rate of prey species. The region of stability of E_1 has been shown in the Figures 6 (red shaded region). The following theorem describes the local asymptotic stability of the boundary equilibrium point E_1.

Theorem 3.2. *The semi-trivial equilibrium point $E_1(\frac{r_0-\delta_1}{\gamma}, 0)$ is locally asymptotically stable if $\delta_1 < r_0 < \delta_1 + \frac{\delta_2\gamma}{\theta\beta - \delta_2\xi}$ with $\theta > \frac{\delta_2\xi}{\beta}$.*

From the biological view point, it is more important to study the local asymptotic stability of the positive interior equilibrium point $E^*(N^*, P^*)$ in which all the interacting species are coexists. In order to study the stability of the singular point $E^*(N^*, P^*)$, we analyze the characteristic equation of the Jacobian matrix for the model (6) is given by

$$\lambda^2 + \left(\gamma N^* - \frac{\beta\xi N^*P^*}{(1+\xi N^*)^2}\right)\lambda + \frac{\theta\beta P^*}{(1+\xi N^*)^2}\left(\frac{\beta N^*}{1+\xi N^*} + \frac{r_0\alpha N^*(1-\eta)}{(\alpha+P^*)^2}\right) = 0,$$

which can be written as

$$\lambda^2 + \rho_{11}\lambda + \rho_{22} = 0, \tag{9}$$

where $\rho_{11} = \gamma N^* - \frac{\beta\xi N^*P^*}{(1+\xi N^*)^2}$ and $\rho_{22} = \frac{\theta\beta P^*}{(1+\xi N^*)^2}\left(\frac{\beta N^*}{1+\xi N^*} + \frac{r_0\alpha N^*(1-\eta)}{(\alpha+P^*)^2}\right)$. From these expressions it is quite difficult to explain the outcomes in terms of ecological system. Thus, we explore this results numerically. Due to Routh-Hurwitz criteria a set of necessary and sufficient conditions for the characteristic roots of (9) will have negative real parts if $\rho_{11} > 0$ and $\rho_{22} > 0$, which gives $\frac{\beta\xi P^*}{\gamma} < (1+\xi N^*)^2$ and $(1+\xi N^*) < \frac{\beta(\alpha+P^*)^2}{r_0\alpha(\eta-1)}$ respectively. The region of stability of E^* has been shown in Fig. 6 (blue shaded region). Therefore, we have the following theorem.

Theorem 3.3. *The necessary condition for the model (6) to be locally asymptotically stable around the coexisting singular point $E^*(N^*, P^*)$ is that $(1+\xi N^*) \in \left(\sqrt{\frac{\beta\xi P^*}{\gamma}}, \frac{\beta(\alpha+P^*)^2}{r_0\alpha(\eta-1)}\right)$.*

3.3. Existence and uniqueness of limit cycle

Existence and stability of a limit cycle in the dynamics of a predator-prey relationships, is related to the existence and stability of biologically feasible singular point(s). We have already shown that our model system (6) exhibits at most two positive interior equilibrium points, otherwise the predator species tend to extinction. If the singular point is stable asymptotically, there may exist limit cycles, the innermost of which must be unstable from the inside and the outermost of which must be stable from the outside or vice-versa. In this case, we will show that if the limit cycle does not exists, the interior singular point is stable globally. If the nonnegative singular point exists and is unstable, there must occur at least one limit cycle. We will employ the approach of Kuang and Freedman (1988) to verify the existence and uniqueness of limit cycles for the model (6), without cost of fear for prey species due to predator population. In order to do that we rewrite the model (6) without cost of fear as

$$\begin{aligned} \frac{dN}{dt} &= Ng(N) - PH(N), \quad \text{with} \quad N(0) \geq 0, \\ \frac{dP}{dt} &= P(-\delta_2 + Q(N)), \quad \text{with} \quad P(0) \geq 0, \end{aligned} \tag{10}$$

where, $g(N) = (r_0 - \delta_1) - \gamma N = \rho - \gamma N$, $H(N) = \frac{\beta N}{1+\xi N}$ and $Q(N) = \frac{\theta\beta N}{1+\xi N}$. The following assumptions are consistent with the model (6) of our predator-prey system with $N, P \geq 0$.

(A1) $g(0) > 0$; there exists a real number $K > 0$ in such a way that $g(N) > 0$ on the interval $0 \leq N < K$.

(A2) $H(0) = 0$, $H'(N) > 0$.

(A3) $Q(0) = 0$, $Q'(N) > 0$.

Theorem 3.4. *Suppose the model system (10) $\frac{d}{dN}\left[\frac{Ng'(N) + g(N) - Ng(N)\frac{H'(N)}{H(N)}}{-\delta_2 + Q(N)}\right] \leq 0$, in the interval $0 \leq N < N^*$ and $N^* < N \leq K$. Then the model system (10) admits exactly one limit cycle which is stable globally with respect to the set $\{(N, P): N > 0, P > 0\}$ $\{E^*(N^*, P^*)\}$.*

To study the existence and uniqueness of limit cycle and the stability of limit cycle, we use the above Theorem 3.4 of our proposed model

(10) without any cost of fear for the prey species due to predator population.

Theorem 3.5. *Suppose that* $r_0 \geq \delta_1 + \gamma\left(2N^* + \frac{1}{\xi}\right)$, *then the model system (10) admits exactly one limit cycle which is stable globally.*

Proof. The proof of this theorem is given in Appendix B. □

Note: It can be observed that whenever the nontrivial singular point for (10) is unstable, then the entire solutions for (10) initiating in the interior of the nonnegative octant of the N-P plane, except at the singular point, approaches a unique limit cycle eventually.

3.4. Analysis of Hopf bifurcation

The possibility of the Hopf bifurcation at an interior singular point $E^*(N^*, P^*)$ has been analyzed here by taking prey birth rate r_0, as a bifurcation parameter and keeping rest of the parameters are constant. To investigate the nature of the interior singular point $E^*(N^*, P^*)$ we required to investigate the sign of the real parts for the characteristic roots of the Eq. (9). A necessary condition for the change of stability for the singular point E^* is that at the characteristic polynomial (9) should have purely complex roots. Roots for the polynomial (9) will be purely complex if $\rho_{11} = 0$ and $\rho_{22} > 0$.

At $\rho_{11} = 0$ gives $P^* = \frac{\gamma(1+\xi N^*)^2}{\xi\beta}$ and (N^*, P^*) satisfies the characteristic Eq. (9). Putting this value of P^* into the characteristic Eq. (9), we get the threshold value of $r_0 = r_0^* = \left(\delta_1 + \frac{\gamma}{\xi} + 2\gamma N^*\right)\left[\frac{\alpha\beta\xi + \gamma(1+N^*)^2}{\alpha\beta\xi + \eta\gamma(1+N^*)^2}\right]$ where $N^* = \frac{\delta_2}{\theta\beta - \xi\delta_2}$.

Let $\lambda(r_0) = \pi_1(r_0) + i\pi_2(r_0)$ be the eigenvalues for the characteristic polynomial (9). Putting this expression into (9) and separating the real and complex parts, we have

$$\begin{aligned} \pi_1^2 - \pi_2^2 + \rho_{11}\pi_1 + \rho_{22} &= 0, \\ 2\pi_1\pi_2 + \rho_{11}\pi_2 &= 0. \end{aligned} \tag{11}$$

Setting $r_0 = r_0^*$ in such a way that $\pi_1(r_0^*) = 0$ and substitute into the Eqs. (11), we have

$$\begin{aligned} -\pi_2^2 + \rho_{22} &= 0, \\ \rho_{11}\pi_2 &= 0, \quad \text{with} \quad \pi_2 \neq 0. \end{aligned} \tag{12}$$

From the above expressions (12), we have $\rho_{11}(r_0^*) = 0$ and $\pi_2(r_0^*) = \sqrt{\rho_{22}(r_0^*)}$, which implies $\lambda(r_0^*) = -i\sqrt{\rho_{22}(r_0^*)}$.

Theorem 3.6. *The necessary and sufficient conditions for the system (6) undergoes Hopf bifurcation from the interior singular point* $E^*(N^*, P^*)$ *is that there exists* $r_0 = r_0^*$ *such that*

(i) $\pi_1(r_0^*) = 0$,

(ii) $\left[\frac{dRe(\lambda(r_0))}{dr_0}\right]_{r_0 = r_0^*} \neq 0.$

Proof. The proof of this theorem is given in Appendix C. □

3.5. Direction and stability of Hopf bifurcation

In the previous subsection, we derived the conditions under which the model (6) experiences Hopf bifurcation. Now, we shall employ center manifold theorem and normal form theory to investigate the direction of Hopf bifurcation and sufficient conditions for the stability of bifurcating periodic solutions arising through Hopf bifurcation. Center manifold theorem is a viable tool in reducing the dimension of a system of differential equations in the neighborhood of coexisting singular point (Guckenheimer and Holmes, 1983; Hassard et al., 1981). We have the following theorem.

Theorem 3.7. *Let,* $\rho_{11}\frac{d\rho_{22}}{dr_0} + 2\pi_2^2\frac{d\rho_{11}}{dr_0} \neq 0$ *then*

1. *the interior equilibrium point* $E^*(N^*, P^*)$ *for (6) is locally asymptotically stable when* $r_0 < r_0^*$ *and unstable when* $r_0 > r_0^*$. *The system (6) experiences a Hopf bifurcation at the nonnegative singular point* $E^*(N^*, P^*)$ *for* $r_0 = r_0^*$.
2. *If* $L'(r_0^*) > 0$ *and* $a(r_0^*) < 0$, *the Hopf bifurcated periodic solutions are stable and the direction of Hopf bifurcation become supercritical.*
3. *If* $L'(r_0^*) > 0$ *and* $a(r_0^*) > 0$, *the Hopf bifurcated periodic solutions are unstable and the direction of Hopf bifurcation become subcritical.*

Proof. Proof of this theorem is given in Appendix D.

4. Numerical simulations

To obtain a better visualization of how different set of parameter values influence the dynamics of the system, in this section we check the feasibility of our analysis regarding the existence of singular points and the corresponding stability conditions numerically, we also solve the model (6) to demonstrate different types of behavior. Most of the parameter values are obtained from Wang et al. (2016) and Wang and Zou (2017), and the rest of system parameters are hypothetical/estimated. Fig. 2 exhibits how the mutual position of the nullclines for the predator-prey model (6) affected by the birth rate r_0 of prey species.

Fig. 3 demonstrates the effect of fear due to predator population on the coexisting equilibrium point E^*. Fig. 3 represents the dependence of the level of fear α and the minimum cost of fear η due to predator species on the birth rate of the prey species r_0, when computed at an interior singular point E^*. It can be observed that the prey species get more fear of the spreading of predator population due to a higher level of the cost of fear, this leads to the larger equilibrium value of the total prey population N which, in turn, results in a maximum level of application of resources, which shows to the decrease in a equilibrium level of the prey birth rate r_0 and a lower level of the minimum cost of fear η. It must be observed, however, that this fear effect is only important for lower level of α, and more increase in the level of fear stemming from perceiving predator population does not result in any important changes in the birth rate of prey species. To gain a better perception into the effects of fear on the interior equilibrium E^*, we plot the Fig. 4 for the equilibrium values of the prey and predator species depending on the prey birth rate r_0 and the conversion coefficient θ. As anticipated, for larger values of r_0 and θ corresponding to the larger values of the equilibrium state prey species, and a lower value of the predator species. For a specific choice of parameter values in this diagram, the interior equilibrium state become stable for any combination of r_0 and θ values observed.

Fig. 5 shows the variability of equilibrium densities of prey and predator species in presence of fear effect. In the Fig. 5, we have plotted four subfigures to better understand the change of equilibrium densities with respect to prey growth rate r_0 and the conversion coefficient θ between prey and predator population. From the Fig. 5(a) and (b) it can be noticed that for lower birth rate r_0 of prey population does not alter the steady state density of prey population N^* (see Fig. 5(a)), however it increases the steady state density of P^* (see Fig. 5(b)). It can be noted that the expression of the equilibrium density of prey is $\delta_2/(\theta\beta - \xi\delta_2)$ which is independent of prey species growth rate r_0. Thus, the prey equilibrium density N^* remain constant with respect to r_0. This scenario can be interpreted as the well-known top-down control of prey species due to predator species, in which the prey steady state density does not depend on the birth rate of prey species. From the Fig. 5(c) and (d) it can be noticed that the conversion coefficient θ plays a crucial role for the equilibrium densities of prey and predator population. The Fig. 5(c) shows that the prey equilibrium density N^* decreases continuously due to increasing value of the conversion coefficient θ whereas the Fig. 5(d) represents that the predator equilibrium density P^* increases and become a predator steady state for increasing value of of the conversion coefficient θ.

Fig. 6 shows how stability of the biologically feasible equilibrium

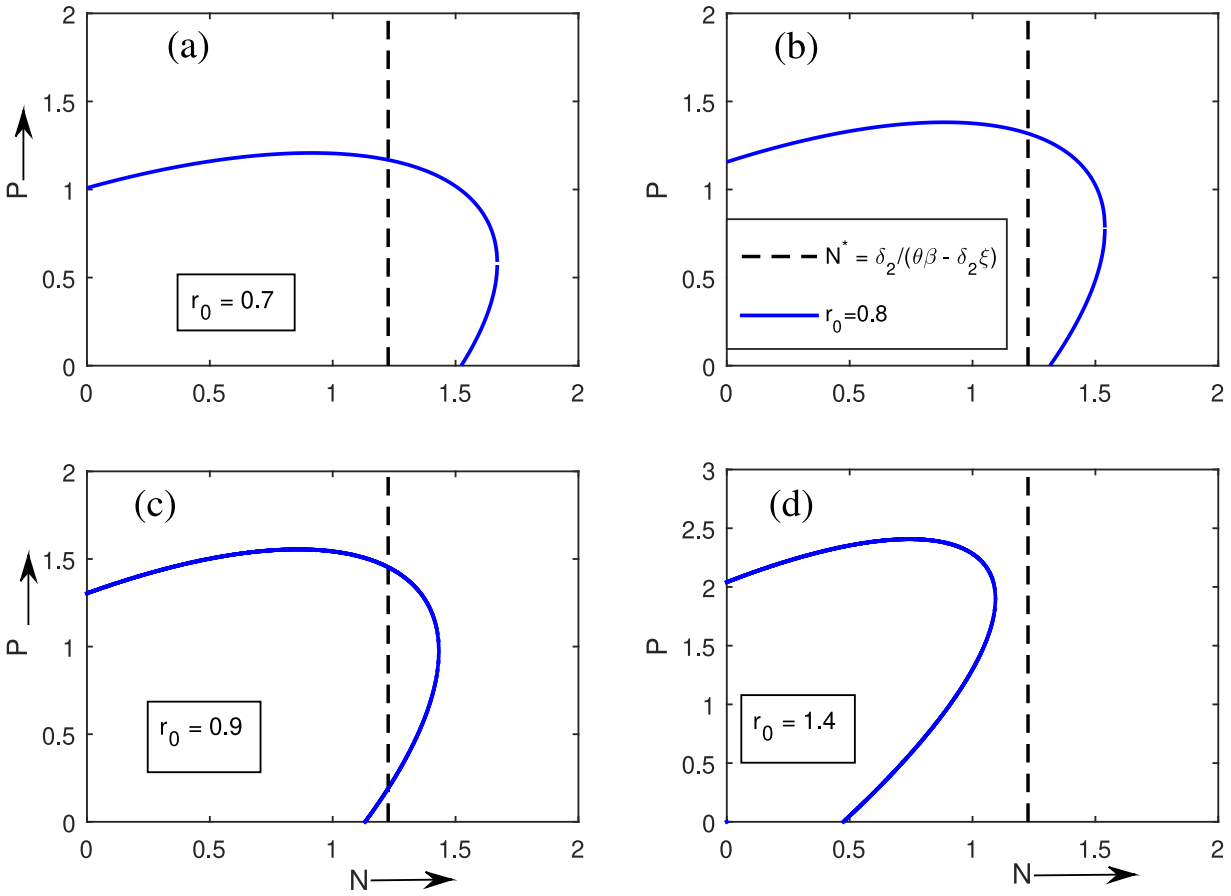

Fig. 2. Mutual position of the nullclines for the predator-prey system (6) with cost of fear and Holling type-II response function. We fixed the parameter values $\eta = 0.10, \alpha = 0.20, \delta_1 = 0.015, \gamma = 0.01, \beta = 0.50, \xi = 0.60, \theta = 0.40, \delta_2 = 0.05$. The figure (a) depicts a unique interior equilibrium point for the model (6) with $r_0 = 0.7$; (b) depicts a unique interior equilibrium point for the model (6) with $r_0 = 0.8$; (c) depicts two interior equilibrium points for the model (6) with $r_0 = 0.9$; (d) depicts the non-existence of interior singular point for the model (6) with $r_0 = 1.4$.

state depends on the relation among r_0 and two rates of positive constants, namely death rate of predators δ_2 and the Michaelis-Menten constant ξ. One observes that for very small value of r_0, the extinct steady state E_0 is locally asymptotically stable for $r_0 < \delta_1$, which has been observed in the green shaded region. The red colored region designates the local asymptotic stability of the predator extinct equilibrium point E_1. Form the Fig. 6 it can be noticed that for larger value of death rate (δ_2) of predator species can be extinct which is a good agreement with the reality as the higher mortality rate always harmful for any kind of species. The blue colored region designates the stability region for E^* in which all the two populations can exists together. The black shaded region designates the instability of all the three biologically feasible equilibrium points. Here the black shaded region is denoted by $E_0^u \cup E_1^u \cup E^{*u}$ in which the three equilibrium points E_0, E_1 and E^* are loses their stability. The parameter values for this simulations are same as in the Fig. 2.

The most important parameters characterizing the dynamics of predator-prey relationship is the growth rate r_0 of prey population and

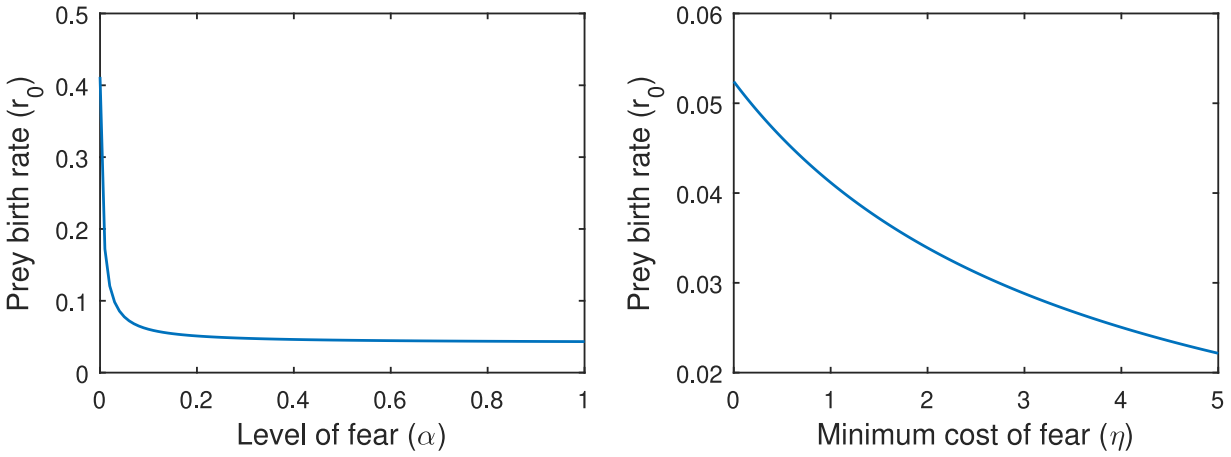

Fig. 3. The figure shows the dependence of the level of fear α and the minimum cost of fear η on the birth rate r_0 of prey populations at the interior singular point $E^*(N^*, P^*)$. The set of parameter values are the same as in Fig. 2.

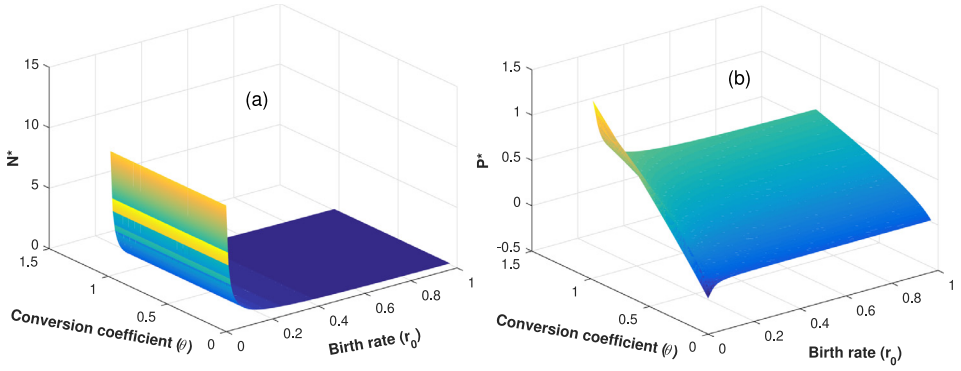

Fig. 4. The figure shows the dependence of the equilibrium state values of the prey and predator populations on the birth rate r_0 of prey populations and the conversion coefficient θ. The set of parameter values are specified in the Fig. 2.

the predators natural mortality rate δ_2, Figs. 7 and 9 represents the Hopf bifurcation diagram for an interior equilibrium state E^* depending on r_0 and δ_2 respectively. For very small values of r_0, and, in agreement with the Theorem 3.1, the trivial singular point E_0 is stable, and the predator extinct singular point E_1 is not biologically feasible. In agreement with Theorem 3.2, if E_1 is locally asymptotically stable then E_0 is unstable, and the interior singular point E^* is biologically meaningful. If we increase the value of r_0, the trivial singular point E_0 loses its stability, and a stable interior equilibrium state occurs. For higher values of r_0, E^* becomes unstable via Hopf bifurcation, shows a stable periodic behavior. Fig. 7 also demonstrates minima and maxima of this solution, indicating the amplitude of oscillations itself increases for r_0, with the lower values for the species on a periodic orbit being very near to zero. From the Fig. 7 it can be noticed that, when r_0 crosses the threshold value $r_0^{[c]} \approx 0.036$, steady state values of prey and predator populations are divided into maximum and minimum of periodic solution and interior steady state becomes unstable in nature. It can be noted that for sufficiently lower values for the prey growth rate r_0, it is possible to attain the situation in which the prey species can live without fear from predators. Fig. 9 represent the Hopf bifurcation diagram for the system (6) with respect to natural mortality rate of predator species δ_2 and other parameters are same as in the Fig. 2. We notice that the model (6) alters the stability from limit cycle behavior to the equilibrium state as the bifurcating parameter increase through the bifurcation point ($\delta_2^{[c]} \approx 0.085$). For $\delta_2 < 0.085$, the model (6) exhibits limit cycle oscillations and the system enters to stable equilibrium state with $\delta_2 > 0.085$ through Hopf bifurcation. Both the Figs. 7 and 9 clearly demonstrates that the prey growth rate r_0 and predators death rates acts as the control parameter.

Fig. 8 represents various dynamical regimes which can be demonstrated for the system (6), beginning with a stable predator free equilibrium state for sufficiently lower value of prey growth rate r_0. For sufficiently larger prey growth rate r_0, we notice that the alteration to a stable interior equilibrium state, with oscillatory approach to this equilibrium state, demonstrating that the maximal characteristic eigenvalues are actually a pair of imaginary eigenvalues with real part negative, that is increasing with r_0. As r_0 passes the critical for a Hopf bifurcation stated in the Theorem 3.6, the model system undergoes on a

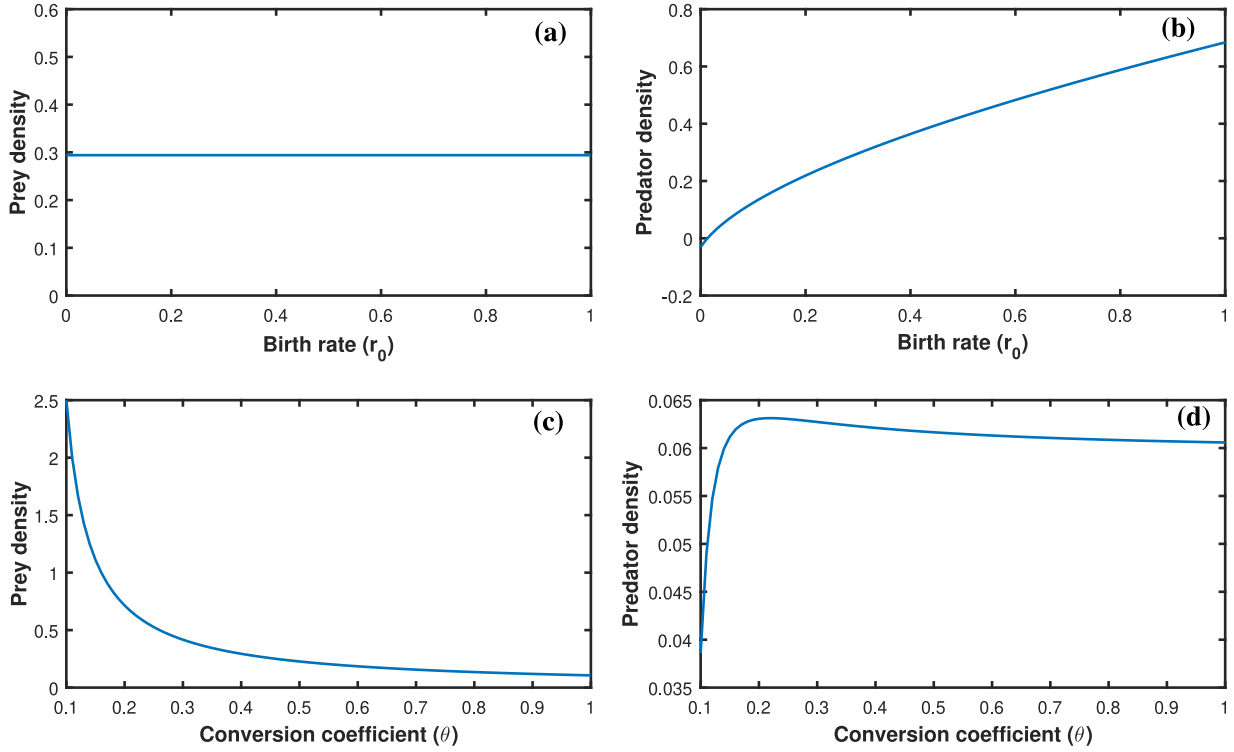

Fig. 5. Change of the equilibrium points for the system (6) with respect to the birth rate r_0 of prey population and conversion coefficient θ. The set of parameters are the same as in the Fig. 2.

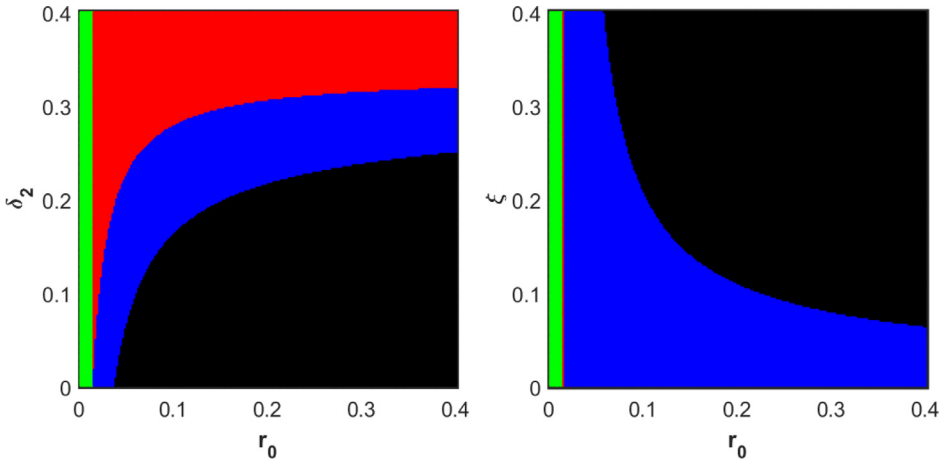

Fig. 6. The figure shows the stability regions for the extinct singular point $E_0(0, 0)$, predator free singular point $E_1(3.5, 0)$ and the co-existing singular point $E^*(0.0294, 0.0531)$ in the parameter spaces $r_0 - \delta_2$ and $r_0 - \xi$ respectively. The green shaded region is the stability region for the trivial singular point E_0, the red shaded region represents the stability region for the axial singular point E_1, the blue shaded region designates the stability region for the interior singular point E^*, whereas the black region is the unstable region for the union of all the equilibrium points, which can be denoted by $E_0^u \cup E_1^u \cup E^{*u}$. We varied both the parameters r_0, δ_2 and ξ from 0 to 0.4 with the initial conditions $[N(0), P(0)] = [0.5, 0.3]$ and other parameters are same as in the Fig. 2. (For interpretation of the references to color in text, the reader is referred to the web version of this article.)

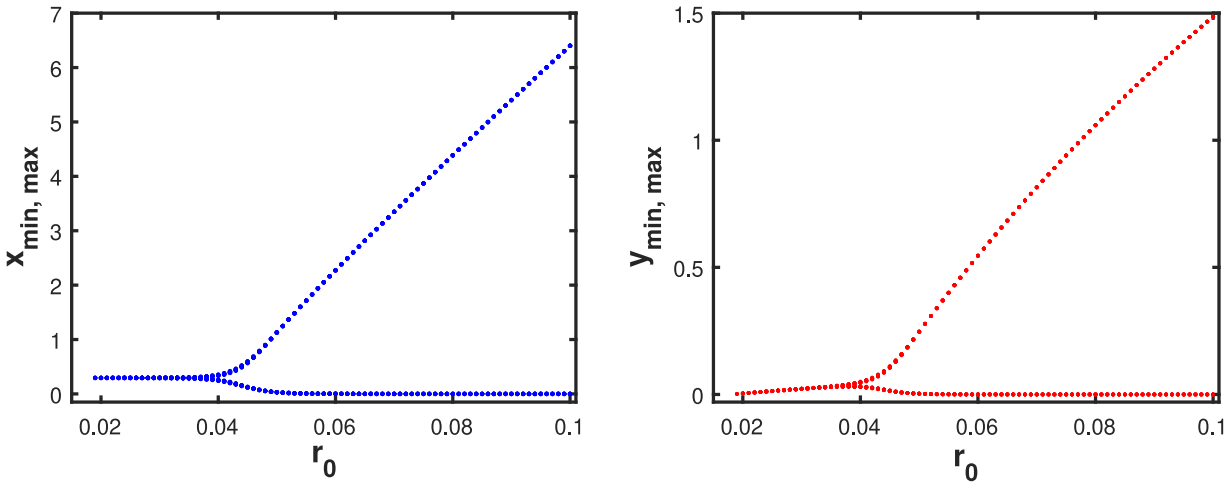

Fig. 7. The figure represents the Hopf bifurcation diagram for the interior singular point E^* of the system (6) considering r_0 as a bifurcation parameter and other parameters are specified in the Fig. 2. We plotted the steady state values of the predator-prey population and the maximum/minimum of the periodic solutions whenever it exists.

stable periodic solution. The corresponding phase diagram also plotted in the Fig. 8(c) for locally asymptotic stable (at $r_0 = 0.03$ in blue color), Fig. 8(d) for periodic solution (at $r_0 = 0.05$ in red color) and Fig. 8(e) for periodic solution with large amplitude (at $r_0 = 0.07$ in black color). Fig. 10 demonstrates various dynamical regimes which can be demonstrated by the system (6), beginning with a large periodic solution for the interior steady for sufficiently small value of predator mortality rate δ_2. For sufficiently larger predators death rate δ_2, we notice that the transition to a periodic solution for interior equilibrium state, with a stable approach to this equilibrium point, indicating the maximal characteristic eigenvalues are actually a pair of imaginary eigenvalues with real part negative become a stable steady state, which is increasing with δ_2. The corresponding phase diagram also plotted in the Fig. 10(c) for large periodic oscillations (at $\delta_2 = 0.03$ in black color), Fig. 10(d) for periodic oscillation (at $\delta_2 = 0.06$ in red color) and Fig. 10(e) for locally asymptotically stable solution (at $r_0 = 0.09$ in blue color).

Considering the parameters values as specified in the Fig. 2, we have computed the values of $L'(r_0{}^*)$ and $a(r_0{}^*)$ with $r_0{}^* = 0.5$ and we get $\Lambda = 0.4718 > 0$ and $a(r_0{}^*) = -0.0221 < 0$. So, according to the Theorem 3.7, the direction of Hopf bifurcation is supercritical. The phase portrait with the same parameters values have been plotted in Fig. 11 with three different initial points. Two initial points are inside the limit cycle and one initial point from the outside of the limit cycle. For all the initial points, the periodic solutions converges to the limit cycle. Hence the direction of the Hopf bifurcation is supercritical.

5. Conclusion

In this paper we have investigated the dynamics of predator-prey system that has introduced the affect that the fear for predator population have on prey population with Holling type II functional response. For the predator-prey system with Holling type II functional response, the cost of fear due to predator species has influenced the predator-prey relationships in several ways. We performed local asymptotic stability analysis of the biologically meaningful singular points, Hopf bifurcation analysis, existence and uniqueness of limit cycle, direction and stability of Poincare-Andronov Hopf bifurcation, analytically. Analytical conditions for local stability analysis and bifurcations for the predator-free and interior equilibrium points have illuminated the role played by different parameter values in obtaining the results of predator-prey

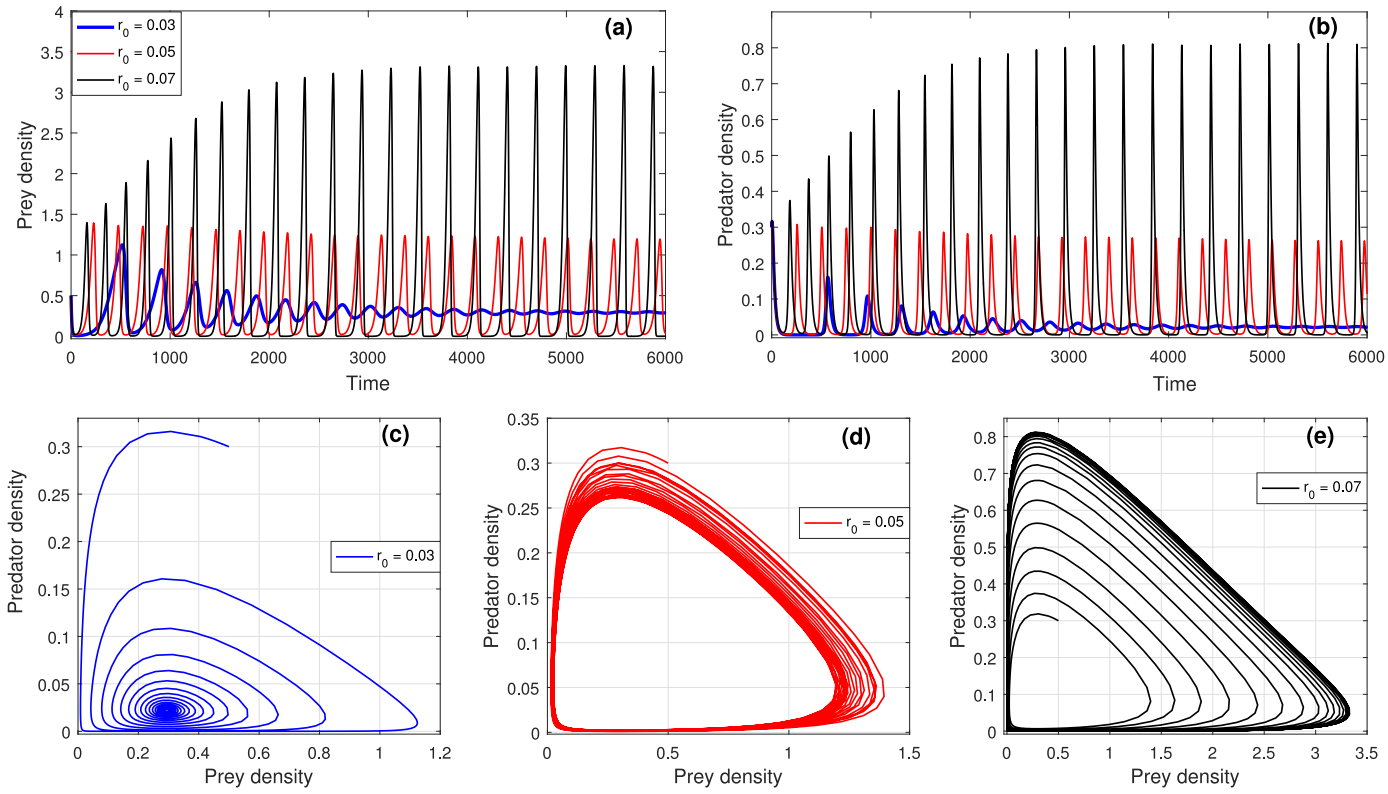

Fig. 8. Numerical solution for the model (6) with parameter values as specified in the Fig. 2: a locally asymptotically stable interior steady state ($r_0 = 0.03$, blue color); periodic solutions around interior equilibrium state ($r_0 = 0.05$, red color), and periodic oscillations with large amplitude around the interior equilibrium state ($r_0 = 0.07$, black color). (For interpretation of the references to color in this figure legend, the reader is referred to the web version of this article.)

system, specifically from the viewpoint of the cost of fear for prey due to predators. Interestingly, complete predator extinction, as characterized by a stable predator-free equilibrium state, cannot be obtained purely by increasing growth rate r_0 of prey species appearing from a consideration of the cost of fear. It can be obtained, though, by increasing the growth rate r_0 of prey population due to predator population, that results in a larger value of prey species growth rate at the predator-free equilibrium state, and the associated higher level of cost-effectiveness.

Analytical findings demonstrate that there exists a locally asymptotically stable nonnegative steady state if the growth rate r_0 of prey population is not high enough to maintain fluctuations. Thus, in this situation both the prey and predator species eventually tend to produce nonnegative constants, no matter how sensitive the prey population is to potential dangers the predator population. For larger prey growth rate r_0, we investigate that the transition to a locally asymptotically stable interior equilibrium, with oscillatory approach to this equilibrium point, indicating that the maximum characteristics eigenvalues are actually a pair of imaginary eigenvalues with real part negative, which is increasing with high level of fear (see the Fig. 7). Therefore, the cost of fear has an impact to stabilize the prey-predator interactions by ruling out periodic oscillatory behavior. This suggests a new interesting technique to ignore the "paradox of enrichment" in ecological system. It is biologically as well as ecologically meaningful and in good agreement with the reality, because after certain level of fear, the prey population become perceive and show signs of habituation. The model

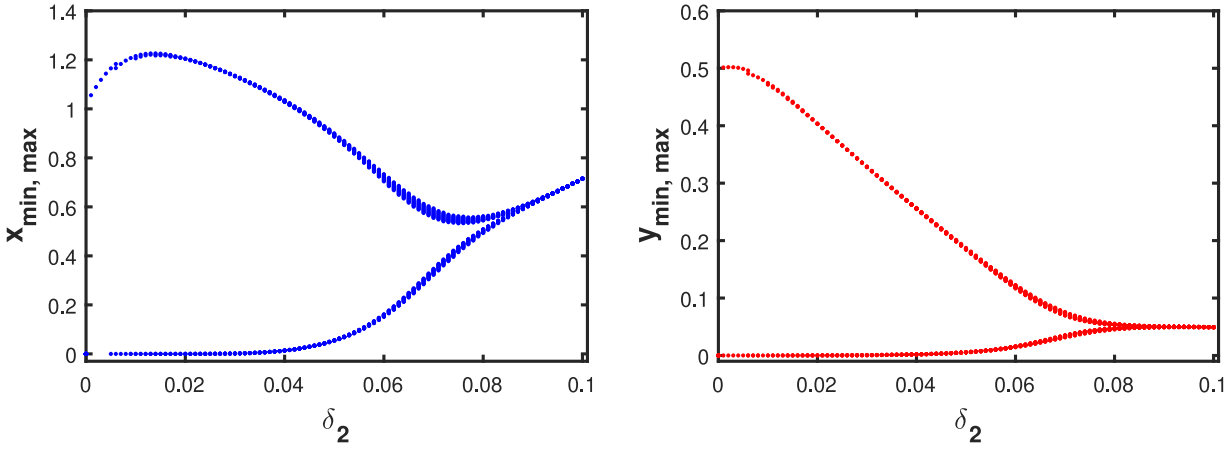

Fig. 9. The figure represents the Hopf bifurcation diagram for the interior singular point E^* of the model (6) considering δ_2 as a bifurcation parameter and other parameters are specified in the Fig. 2. We plotted the steady state values of the predator-prey population and the maximum/minimum of the periodic solutions whenever it exists.

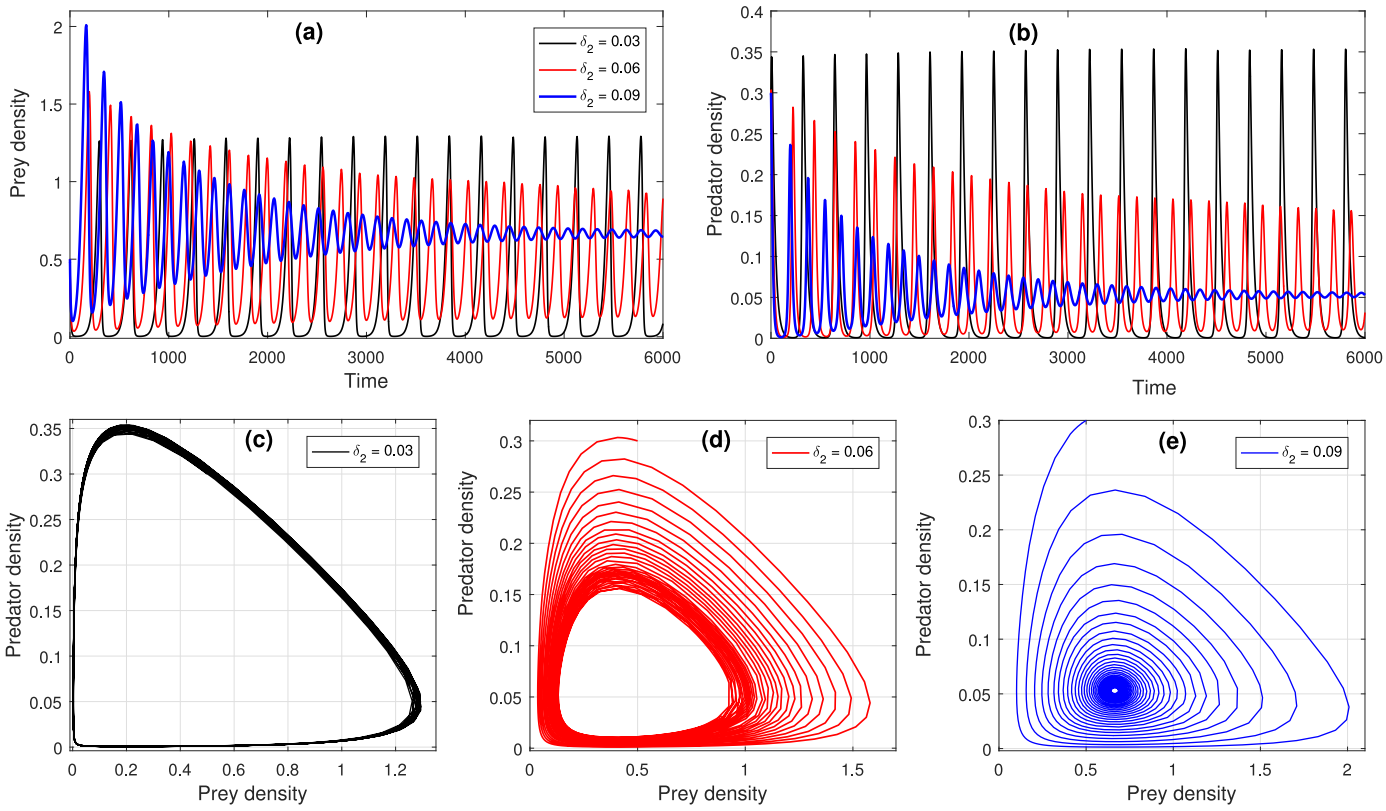

Fig. 10. Numerical solution for the model (6) with parameter values as specified in the Fig. 2: periodic oscillations with large amplitude around the interior equilibrium state ($\delta_2 = 0.03$, black color); periodic solutions around interior equilibrium state ($\delta_2 = 0.06$, red color), and a stable solution around the interior equilibrium state ($\delta_2 = 0.09$, black color). (For interpretation of the references to color in this figure legend, the reader is referred to the web version of this article.)

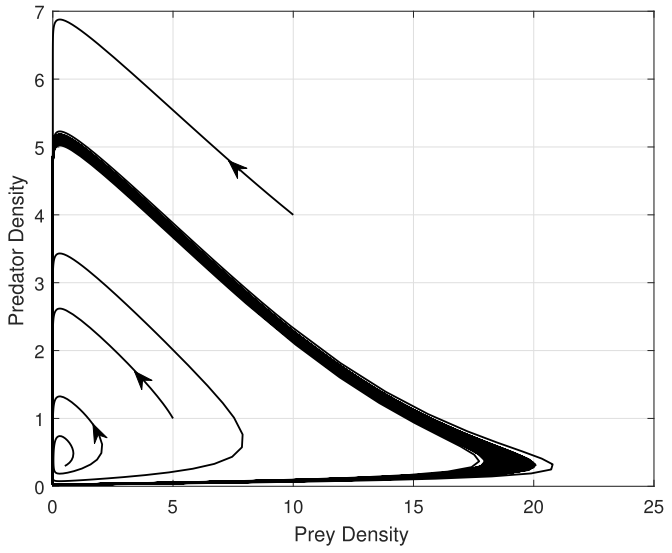

Fig. 11. Numerical solution for the model (6) with parameter values as specified in the Fig. 2 and $r_0 = 0.5$. Periodic solution around the interior equilibrium $E^*(0.2941, 0.4181)$ shows supercritical Hopf bifurcation.

system under consideration exhibits that the periodic oscillations can persist for the low level of prey birth rate r_0 (see the bifurcation Fig. 7 and the time series solution and phase-portrait diagram Fig. 8). We investigate the situations for the occurrence of Hopf bifurcation and the conditions for investigating the direction of Poincare-Andronov Hopf bifurcation, which demonstrate that the cost of fear will not only influence the occurrence of Hopf bifurcation but also alter the direction of Poincare-Andronov Hopf bifurcation, in agreement with Theorem 3.7.

We have verified that the Hopf bifurcation in the model introducing the cost of fear can be both subcritical or supercritical according to the sign of the coefficient of $a(r_0^*)$ (see the Theorem 3.7).

We performed some numerical simulations to investigate the potentiality that the cost of fear can play a pivotal role in predator-prey systems. We observed that the prey growth rate r_0 and natural mortality rate for predators δ_2 can exhibit bistability situation by creating multiple limit cycles via subcritical Hopf bifurcation. By increasing the prey growth rate r_0 may cause the alter in the direction of Poincare-Andronov Hopf bifurcation, according to the sign of the coefficient of $a(r_0^*)$ from supercritical to subcritical. From the bifurcation diagram (see Fig. 9) and the numerical solution (see Fig. 10(a)-(e)) it can be observed that for increasing the predator mortality rate δ_2 there is a transition to a stable periodic oscillation from a stable interior singular point, indicating the characteristic eigenvalues are actually a pair of imaginary roots with real part negative from the eigenvalues are real and negative, which is increasing with δ_2. Due to fear, the prey birth rate r_0 develops rich dynamical behavior including bi-stability, in which the solutions tend to a periodic oscillatory behavior from stable steady state depending on the initial size of the population. Similarly, due to fear the predator mortality rate δ_2 develops rich dynamical behavior including bi-stability, in which the solutions tend to a stable equilibrium state from periodic oscillatory behavior depending on the initial size of the population. Model simulations also exhibit that the prey species are less sensitive to perceive predation risk when the prey growth rate r_0 become larger, irrespective of how other parameter values alter. Furthermore, the prey species would be more willing to exhibit anti-predator defences when the rate of predation become larger. Model simulations regarding the cost of fear represent that the outcomes we have obtained in this manuscript, sincerely hope that it will be helpful for further study/investigation.

In the model formulation we have considered the predator-prey

relationship by introducing the role of fear effect with Holling type II response function. We consider the mathematical model depicting predator-prey system studied by Wang et al. (2016) as the base framework. Here we studied the case in which the intra-specific competition for the prey population is not influenced by fear due to predator population. There are some theoretical argument that the effect of fear may alter the strength of intra-specific competition for prey population because of the complexity of food web model (Cresswell, 2011). Zanette et al. (2011) experimentally investigated that the fear of predation risk can reduce the reproduction of song sparrow even in lack of direct killing. In our model, we focused discerned predation risks only decrease the prey growth rate and survival of off-spring, and avoid the viable influence for the mortality rate of prey. Zanette et al. (2011) argue that the cost of fear has an effect on the death rate of prey due to long-run physiological effects, but there is a lack of observational proof. Once we get some experimental confirmation, these should all be introduced into the predator-prey system, and such a model would be able shed more light on the predator-prey system. To make the model more realistic, we can also be refined to introduce mutual interference and prey defense.

Declaration of Competing Interest

The authors declare that there is no conflict of interests regarding the publication of this manuscript.

Acknowledgment

We are grateful to the anonymous reviewers for their comments and useful suggestions to improve the quality of the paper. This study of Subhas Khajanchi was partially supported by the Indo French Centre for Applied Mathematics (IFCAM) (Grant No. MA/IFCAM/18/50).

Appendix A

Proof of the Lemma 2.1.

Proof. To prove the boundedness of the system (6), we consider the function

$$\psi(t) = N(t) + \frac{1}{\theta}P(t).$$

The time derivative along the solution trajectories for the model (6) is

$$\begin{aligned}\frac{d\psi(t)}{dt} &= \frac{dN(t)}{dt} + \frac{1}{\theta}\frac{dP(t)}{dt}\\ &= r_0 N\left[\eta + \frac{\alpha(1-\eta)}{\alpha + P}\right] - \delta_1 N - \gamma N^2 - \frac{\delta_2}{\theta}P\\ &\leq r_0 N(\eta + (1-\eta)) - \delta_1 N - \gamma N^2 - \frac{\delta_2}{\theta}P.\end{aligned}$$

Now, for each $\psi(t) > 0$, we get

$$\frac{d\psi(t)}{dt} + \rho\psi(t) \leq r_0 N(t) - \gamma N^2,$$

where $\rho = \min\{\delta_1, \frac{\delta_2}{\theta}\}$. The maximum value of $r_0 N(t) - \gamma N^2$ is $\frac{r_0^2}{4\gamma}$. Therefore,

$$\frac{d\psi(t)}{dt} + \rho\psi(t) \leq \frac{r_0^2}{4\gamma} = \lambda \text{ (say)}.$$

Now, applying the theory of differential inequality for $\psi(t)$, we have

$$0 < \psi(N, P) \leq \frac{\lambda}{\rho}(1 - e^{-\rho t}) + \psi(N(0), P(0))e^{-\rho t},$$

and for $t \to +\infty$, we obtain $0 < \psi \leq \frac{\lambda}{\rho}$. Hence, all the solutions for the system (6), which initiating in R_+^2 are confined in the region

$$\Omega = \left\{(N, P) \in R_+^2 : \psi = \frac{\lambda}{\rho} + \epsilon, \text{ for any } \epsilon > 0\right\}.$$

This shows that the solutions of the system represented by the Eq. (6) is bounded. □

Appendix B

Proof of the Theorem 3.5.

Proof. To prove the theorem, we employ the Theorem 3.4 by Kuang and Freedman (1988), we have

$$\frac{d}{dN}\left[\frac{Ng'(N)+g(N)-Ng(N)\frac{H'(N)}{H(N)}}{-\delta_2+Q(N)}\right] \le 0$$

$$\Leftrightarrow \frac{d}{dN}\left[\frac{N(-\gamma)+(\rho-\gamma N)-N(\rho-\gamma N).\frac{\beta}{(1+\xi N)^2}.\frac{(1+\xi N)}{\beta N}}{-\delta_2+\frac{\theta\beta N}{1+\xi N}}\right] \le 0$$

$$\Leftrightarrow \frac{d}{dN}\left[\frac{N(-\gamma)+(\rho-\gamma N)-\frac{(\rho-\gamma N)}{1+\xi N}}{-\delta_2+\frac{\theta\beta N}{1+\xi N}}\right] \le 0$$

$$\Leftrightarrow \frac{d}{dN}\left[\frac{N(-\gamma)+(\rho-\gamma N)\frac{\xi N}{1+\xi N}}{-\delta_2+\frac{\theta\beta N}{1+\xi N}}\right] \le 0$$

$$\Leftrightarrow \frac{d}{dN}\left[\frac{\xi N(\rho-\gamma N)+(1+\xi N)(-N\gamma)}{\theta\beta N-\delta_2(1+\xi N)}\right] \le 0$$

$$\Leftrightarrow \frac{d}{dN}\left[\frac{\xi N(\gamma N-\rho)+N\gamma(1+\xi N)}{\theta\beta N-\delta_2(1+\xi N)}\right] \ge 0$$

$$\Leftrightarrow \frac{d}{dN}\left[\frac{\xi N(\gamma N-\rho)+N\gamma(1+\xi N)}{(\theta\beta-\delta_2\xi)(N-\Delta)}\right] \ge 0, \quad \text{where } \Delta = \frac{\delta_2}{\theta\beta-\delta_2\xi} = N^*$$

$$\Leftrightarrow \frac{d}{dN}\left[\frac{\xi\gamma}{(\theta\beta-\delta_2\xi)}.\frac{N\left(2N+\frac{1}{\xi}-\frac{\rho}{\gamma}\right)}{N-\Delta}\right] \ge 0$$

$$\Leftrightarrow \frac{d}{dN}\left[\frac{N\left(2N+\frac{1}{\xi}-\frac{\rho}{\gamma}\right)}{N-\Delta}\right] \ge 0$$

$$\Leftrightarrow \left(2N+\frac{1}{\xi}-\frac{\rho}{\gamma}+2N\right)(N-\Delta)-N\left(2N+\frac{1}{\xi}-\frac{\rho}{\gamma}\right) \ge 0$$

$$\Leftrightarrow 2N^2-4N\Delta-\Delta\left(\frac{1}{\xi}-\frac{\rho}{\gamma}\right) \ge 0$$

$$\Leftrightarrow (N-\Delta)^2+\frac{\Delta}{2}\left(\frac{\rho}{\gamma}-\frac{1}{\xi}\right)-\Delta^2 \ge 0$$

$$\Leftrightarrow \left(\frac{\rho}{\gamma}-\frac{1}{\xi}\right) \ge 2\Delta$$

$$\Leftrightarrow \rho \ge \gamma\left(2\Delta+\frac{1}{\xi}\right),$$

that is, $r_0 \ge \delta_1+\gamma\left(\frac{2\delta_2}{\theta\beta-\delta_2\xi}+\frac{1}{\xi}\right)$. The equality holds if and only if $r_0=\delta_1+\gamma\left(\frac{2\delta_2}{\theta\beta-\delta_2\xi}+\frac{1}{\xi}\right)$, which implies that the the existence and uniqueness of limit cycle and the global stability depends on the value of prey populations and which also measured by the growth rate of prey population. From which we can conclude that the introduction of the cost of fear for prey species play an important role on the coexistence of predator-prey species. By using the Theorem 3.4, we investigate that for $r_0 \ge \delta_1+\gamma\left(\frac{2\delta_2}{\theta\beta-\delta_2\xi}+\frac{1}{\xi}\right)$, the model system (10) admits only one limit cycle which is stable globally. This completes the proof of the Theorem. □

Appendix C

Proof of the Theorem 3.6.

Proof. The eigenvalues of the characteristic polynomial (9) are given by

$$\lambda_{1,2}=\frac{-\rho_{11}\pm\sqrt{\rho_{11}^2-4\rho_{22}}}{2},$$

where ρ_{11} and ρ_{22} are the functions of the birth rate of prey population r_0, in which all other parameters are fixed. Furthermore, we assume that there exists parameter $r_0=r_0^*$ in such a way that $\rho_{11}(r_0^*)=0$ and $\rho_{22}(r_0^*)>0$. Thus, the nonnegative real roots of these eigenvalues alter the sign when r_0 crosses through the critical value r_0^*. Consequently, the model system (6) switches its stability provided that the transversality condition is assured.

Differentiating both the expressions (11), with respect to r_0 and then substitute $\pi_1(r_0)=0$, we get

$$\begin{aligned}\rho_{11}\frac{d\pi_1(r_0)}{dr_0}-2\pi_2\frac{d\pi_2(r_0)}{dr_0} &= -\frac{d\rho_{22}(r_0)}{dr_0},\\ 2\pi_2\frac{d\pi_1(r_0)}{dr_0}+\rho_{11}\frac{d\pi_2(r_0)}{dr_0} &= -\pi_2\frac{d\rho_{11}(r_0)}{dr_0}.\end{aligned} \tag{13}$$

Solving the above system of Eqs. (13), we get

$$\left[\frac{dRe(\lambda(r_0))}{dr_0}\right]_{r_0=r_0^*} = -\left[\frac{\rho_{11}\frac{d\rho_{22}}{dr_0} + 2\pi_2^2\frac{d\rho_{11}}{dr_0}}{\rho_{11}^2 + 4\pi_2^2}\right]_{r_0=r_0^*} \neq 0,$$

provided $\rho_{11}\frac{d\rho_{22}}{dr_0} + 2\pi_2^2\frac{d\rho_{11}}{dr_0} \neq 0$. This completes the proof. □

Appendix D

Proof of the Theorem 3.7.

Proof. For our present system, given by the Eq. (6), we obtained that the variational matrix $J(N^*, P^*)$ has a pair of purely complex eigenvalues at the Hopf bifurcation point $r_0 = r_0^*$. Thus, we can analyze the model under consideration on a two dimensional center manifold. The flow transverse to the center manifold is relatively simple, that is, exponentially contracting. To investigate the center manifold and investigate the flow theorem, first we translate the nonnegative interior singular point $E^*(N^*, P^*)$ to the origin by using the transformation $\hat{N} = N - N^*$ and $\hat{P} = P - P^*$. For simplicity, we denote $\hat{N}$ and $\hat{P}$ again by N and P respectively. We can rewrite the system of Eq. (6), by Taylor series expansion about (N^*, P^*) as follows

$$\begin{aligned}
\frac{dN}{dt} &= r_0(N+N^*)\left(\eta + \frac{\alpha(1-\eta)}{\alpha + P + P^*}\right) - \delta_1(N+N^*) - \gamma(N+N^*)^2 - \frac{\beta(N+N^*)(P+P^*)}{1+\xi(N+N^*)},\\
\frac{dP}{dt} &= \frac{\theta\beta(N+N^*)(P+P^*)}{1+\xi(N+N^*)} - \delta_2(P+P^*).
\end{aligned} \tag{14}$$

The system (14) can be rewritten as

$$\begin{bmatrix}\frac{dN}{dt}\\ \frac{dP}{dt}\end{bmatrix} = J^*(N^*, P^*)\begin{bmatrix}N\\P\end{bmatrix} + \begin{bmatrix}\phi(N,P)\\ \psi(N,P)\end{bmatrix}, \tag{15}$$

where

$$\begin{aligned}
\phi(N,P) &= a_1N^2 + a_2NP + a_3P^2 + \cdots,\\
\psi(N,P) &= b_1N^2 + b_2NP + b_3P^2 + \cdots,
\end{aligned}$$

with

$$\begin{aligned}
a_1 &= -\gamma + \frac{\beta\xi P^*}{(1+\xi N^*)^2} - \frac{\beta\xi N^*P^*}{(1+\xi N^*)^2},\\
a_2 &= \frac{r_0\alpha(1-\eta)}{(\alpha+P^*)^2} - \frac{\beta}{(1+\xi N^*)} + \frac{\beta\xi N^*}{(1+\xi N^*)^2},\\
a_3 &= \frac{r_0\alpha N^*(1-\eta)}{(\alpha+P^*)^3}, \cdots,\\
b_1 &= \frac{\theta\beta\xi P^*}{(1+\xi N^*)^2} + \frac{\theta\beta\xi^2 N^*P^*}{(1+\xi N^*)^3},\\
b_2 &= \frac{\theta\beta}{1+\xi N^*} - \frac{\theta\beta\xi N^*}{(1+\xi N^*)^2}, \qquad b_3 = 0, \cdots.
\end{aligned}$$

The characteristic roots of $J^*(N^*, P^*)$ are of the form $\lambda_{1,2} = L \pm iM$, where $L = \frac{1}{2}(tr(J^*))$ and $M = \sqrt{\det(J^*) - L^2}$. Here, the eigenvalues λ_1 and λ_2 will be complex conjugate if $\det(J^*) - L^2 > 0$ and λ_1, λ_2 will be purely imaginary at $r_0 = r_0^*$, that is, $L(r_0^*) = 0$ and then $\lambda_{1,2} = \pm iM(r_0^*)$.

The eigenvectors of $J^*(N^*, P^*)$ corresponding to the eigen values of $\lambda = L + iM$ are given by

$$X = \begin{bmatrix}1\\ Y - iZ\end{bmatrix},$$

where

$$\begin{aligned}
Y &= \frac{\theta(\alpha+P^*)^2}{r_0\alpha\theta(1-\eta)N^* + \delta_2(\alpha+P^*)^2}\left(\gamma N^* - \frac{\beta\xi N^*P^*}{(1+\xi N^*)^2} + M\right),\\
Z &= -\frac{\theta(\alpha+P^*)^2 L}{r_0\alpha(1-\eta)\theta N^* + \delta_2(\alpha+P^*)^2}.
\end{aligned}$$

We set the matrix as follows

$$D = \begin{bmatrix}1 & 0\\ Y & Z\end{bmatrix}.$$

By using the transformation

$$\begin{bmatrix} N \\ P \end{bmatrix} = D \begin{bmatrix} x \\ y \end{bmatrix},$$

that is, $N = x$ and $P = xY + yZ$. Using the above transformation the model system (15) becomes

$$\begin{bmatrix} \frac{dx}{dt} \\ \frac{dy}{dt} \end{bmatrix} = J^*(N^*, P^*) \begin{bmatrix} x \\ y \end{bmatrix} + \begin{bmatrix} Q(x, y) \\ R(x, y) \end{bmatrix}, \tag{16}$$

where

$$J^*(N^*, P^*) = \begin{bmatrix} L & -M \\ M & L \end{bmatrix},$$

and

$$\begin{aligned} Q(x, y) &= \left[-\gamma + \frac{r_0\alpha(1-\eta)N^*Y^2}{(\alpha + P^*)^3} - \frac{r_0\alpha(1-\eta)Y}{(\alpha + P^*)^3} - \frac{\beta\xi^2 N^*P^*}{(1+\xi N^*)^3} + \frac{\beta\xi P^*}{(1+\xi N^*)^2} \right. \\ &\quad \left. - \frac{\beta\xi N^*Y}{(1+\xi N^*)^2} - \frac{\beta Y}{1+\xi N^*} \right] x^2 + \left[\frac{r_0\alpha(1-\eta)N^*Z^2}{(\alpha + P^*)^3} \right] y^2 \\ &\quad + \left[-\frac{\beta Z}{1+\xi N^*} + \frac{r_0\alpha(1-\eta)N^*YZ}{(\alpha + P^*)^3} + \frac{r_0\alpha(1-\eta)Z}{(\alpha + P^*)^2} + \frac{\beta\xi N^*Z}{(1+\xi N^*)^2} \right] xy \\ &\quad + \left[-\frac{r_0\alpha(1-\eta)N^*Y^3}{(\alpha + P^*)^4} + \frac{r_0\alpha(1-\eta)Y^2}{(\alpha + P^*)^3} + \frac{\beta\xi^3 N^*P^*}{(1+\xi N^*)^4} - \frac{\beta\xi P^{*2}}{(1+\xi N^*)^3} \right. \\ &\quad \left. - \frac{\beta\xi^2 N^*Y}{(1+\xi N^*)^3} + \frac{\beta\xi Y}{(1+\xi N^*)^2} \right] x^3 + \cdots \end{aligned}$$

$$\begin{aligned} R(x, y) &= \frac{1}{Z}\left[\frac{\theta\beta\xi^2 N^*P^*}{(1+\xi N^*)^3} - \frac{\theta\beta\xi P^*}{(1+\xi N^*)^2} - \frac{\theta\beta\xi N^*Y}{(1+\xi N^*)^2} - \frac{r_0\alpha(1-\eta)N^*Y^3}{(\alpha + P^*)^3} + \frac{r_0\alpha(1-\eta)Y^2}{(\alpha + P^*)^2} \right. \\ &\quad \left. + \gamma Y + \frac{\beta Y^2}{1+\xi N^*} - \frac{\beta\xi P^*Y}{(1+\xi N^*)^2} + \frac{\beta\xi N^*Y^2}{(1+\xi N^*)^2} + \frac{\beta\xi^2 N^*P^*Y}{(1+\xi N^*)^3} + \frac{\theta\beta Y}{1+\xi N^*} \right] x^2 \\ &\quad - \left[\frac{r_0\alpha(1-\eta)YZ}{(\alpha + P^*)^3} \right] y^2 + \left[\frac{\beta Y}{1+\xi N^*} + \frac{\theta\beta}{1+\xi N^*} - \frac{\theta\beta\xi N^*}{(1+\xi N^*)^2} + \frac{r_0\alpha(1-\eta)Y}{(\alpha + P^*)^2} \right. \\ &\quad \left. - \frac{2r_0\alpha(1-\eta)N^*Y}{(\alpha + P^*)^3} - \frac{\beta\xi N^*Y}{(1+\xi N^*)^2} \right] xy + \cdots \end{aligned}$$

The model system (16) can be written in the polar form as

$$\begin{aligned} \frac{dr}{dt} &= L(r_0)r + a(r_0)r^3 + ..., \\ \frac{d\theta}{dt} &= M(r_0) + c(r_0)r^2 + ... \end{aligned} \tag{17}$$

The Taylor's series expansion of (17) at $r_0 = r_0^*$ gives

$$\begin{aligned} \frac{dr}{dt} &= L'(r_0^*)(r_0 - r_0^*)r + a(r_0^*)r^3 + ..., \\ \frac{d\theta}{dt} &= M(r_0^*) + M'(r_0^*)(r_0 - r_0^*) + c(r_0^*)r^2 + ..., \end{aligned} \tag{18}$$

where

$$\begin{aligned} a(r_0^*) &= \frac{1}{16}[Q_{xxx} + Q_{xyy} + R_{xxy} + R_{yyy}]_{(0,0,r_0^*)} \\ &\quad + \frac{1}{16M(r_0^*)}[Q_{xy}(Q_{xx} + Q_{yy}) - R_{xy}(R_{xx} + R_{yy}) - Q_{xx}R_{xx} + Q_{yy}R_{yy}]_{(0,0,r_0^*)} \end{aligned}$$

with

$$
\begin{aligned}
Q_{xxx}(0,0,r_0^*) &= 6\left[-\frac{r_0^*\alpha(1-\eta)N^*Y^3}{(\alpha+P^*)^4}+\frac{r_0^*\alpha(1-\eta)Y^2}{(\alpha+P^*)^3}+\frac{\beta\xi^3N^*P^*}{(1+\xi N^*)^4}-\frac{\beta\xi P^{*2}}{(1+\xi N^*)^3}\right.\\
&\quad\left.-\frac{\beta\xi^2N^*Y}{(1+\xi N^*)^3}+\frac{\beta\xi Y}{(1+\xi N^*)^2}\right],\\
Q_{xyy}(0,0,r_0^*) &= 2\left[-\frac{3r_0^*\alpha(1-\eta)N^*YZ^2}{(\alpha+P^*)^4}+\frac{r_0^*\alpha(1-\eta)Z^2}{(\alpha+P^*)^3}\right],\\
R_{xxy}(0,0,r_0^*) &= 2\left[-\frac{\theta\beta\xi}{(1+\xi N^*)^2}-\frac{\beta\xi Y}{(1+\xi N^*)^2}+\frac{\theta\beta\xi^2N^*}{(1+\xi N^*)^3}+\frac{3r_0^*\alpha(1-\eta)N^*Y^3}{(\alpha+P^*)^4}\right.\\
&\quad\left.-\frac{2r_0^*\alpha(1-\eta)Y^2}{(\alpha+P^*)^3}+\frac{\beta\xi^2N^*Y}{(1+\xi N^*)^3}\right],\\
R_{yyy}(0,0,r_0^*) &= \frac{r_0^*\alpha(1-\eta)N^*YZ^2}{(\alpha+P^*)^4},\\
Q_{xy}(0,0,r_0^*) &= -\frac{\beta Z}{1+\xi N^*}+\frac{2r_0^*\alpha(1-\eta)N^*YZ}{(\alpha+P^*)^3}-\frac{r_0^*\alpha(1-\eta)Z}{(\alpha+P^*)^2}+\frac{\beta\xi N^*Z}{(1+\xi N^*)^2},\\
Q_{xx}(0,0,r_0^*) &= 2\left[-\gamma+\frac{r_0^*\alpha(1-\eta)N^*Y^2}{(\alpha+P^*)^3}-\frac{r_0^*\alpha(1-\eta)Y}{(\alpha+P^*)^3}-\frac{\beta\xi^2N^*P^*}{(1+\xi N^*)^3}\right.\\
&\quad\left.+\frac{\beta\xi P^*}{(1+\xi N^*)^2}-\frac{\beta\xi N^*Y}{(1+\xi N^*)^2}-\frac{\beta Y}{1+\xi N^*}\right],\\
Q_{yy}(0,0,r_0^*) &= \frac{2r_0^*\alpha(1-\eta)N^*Z^2}{(\alpha+P^*)^3},\\
R_{xy}(0,0,r_0^*) &= \frac{\beta Y}{1+\xi N^*}+\frac{\theta\beta}{1+\xi N^*}-\frac{\theta\beta\xi N^*}{(1+\xi N^*)^2}+\frac{r_0^*\alpha(1-\eta)Y}{(\alpha+P^*)^2}\\
&\quad-\frac{2r_0^*\alpha(1-\eta)N^*Y}{(\alpha+P^*)^3}-\frac{\beta\xi N^*Y}{(1+\xi N^*)^2},\\
R_{yy}(0,0,r_0^*) &= -\frac{2r_0^*\alpha(1-\eta)N^*YZ}{(\alpha+P^*)^3},
\end{aligned}
$$

$$
\begin{aligned}
R_{xx}(0,0,r_0^*) &= \frac{2}{Z}\left[\frac{\theta\beta\xi^2N^*P^*}{(1+\xi N^*)^3}-\frac{\theta\beta\xi P^*}{(1+\xi N^*)^2}-\frac{\theta\beta\xi N^*Y}{(1+\xi N^*)^2}-\frac{r_0^*\alpha(1-\eta)N^*Y^3}{(\alpha+P^*)^3}\right.\\
&\quad+\frac{r_0^*\alpha(1-\eta)Y^2}{(\alpha+P^*)^2}+\gamma Y+\frac{\beta Y^2}{1+\xi N^*}-\frac{\beta\xi P^*Y}{(1+\xi N^*)^2}-\frac{\beta\xi N^*Y^2}{(1+\xi N^*)^2}\\
&\quad\left.+\frac{\beta\xi^2N^*P^*Y}{(1+\xi N^*)^3}+\frac{\theta\beta Y}{1+\xi N^*}\right].
\end{aligned}
$$

The sign of the coefficient of $a(r_0^*)$ determines the stability of Hopf bifurcating periodic solution. Thus, we have

$$
\begin{aligned}
\left[\frac{\partial L}{\partial r_0}\right]_{r_0=r_0^*} &= [\text{Derivative of real part of the eigen value with respect to } r_0]_{r_0=r_0^*}\\
&= -\left[\frac{\rho_{11}\frac{d\rho_{22}}{dr_0}+2\pi_2^2\frac{d\rho_{11}}{dr_0}}{\rho_{11}^2+4\pi_2^2}\right]_{r_0=r_0^*}\neq 0,
\end{aligned}
$$

provided $\rho_{11}\frac{d\rho_{22}}{dr_0}+2\pi_2^2\frac{d\rho_{11}}{dr_0}\neq 0$. Thus,

$$\Lambda=-\frac{a(r_0^*)}{L'(r_0^*)}.$$

□

Supplementary material

Supplementary material associated with this article can be found, in the online version, at 10.1016/j.ecocom.2020.100826 .

References

Beddington, J.R., 1975. Mutual interference between parasites or predators and its effect on searching efficiency. J. Anim. Ecol. 44 (1), 331–340.

Chinnathambi, R., Rihan, F.A., 2018. Stability of fractional-order prey-predator system with time-delay and Monod-Haldane functional response. Nonlinear Dyn. 92 (4), 1637–1648.

Creel, S., Christianson, D., 2008. Relationships between direct predation and risk effects. Trends. Ecol. Evol. 23, 194–201.

Creel, S., Christianson, D., Liley, S., Winnie, J.A., 2007. Predation risk affects reproductive physiology and demography of elk. Science 315 (5814), 960.

Cresswell, W., 2011. Predation in bird populations. J. Ornithol. 152 (1), 251–263.

Das, A., Samanta, G.P., 2018. Modeling the fear effect on a stochastic prey-predator system with additional food for the predator. J. Phys. A 51, 465601.

De Angelis, D.L., Goldstein, R.A., O'Neill, R.V., 1975. A model for tropic interaction. Ecology 56 (4), 881–892.

Eggers, S., Griesser, M., Nystrand, M., Ekman, J., 2006. Predation risk induces changes in

nest-site selection and clutch size in the Siberian jay. Proc. R. Soc. B Biol. Sci. 273 (1587), 701–706.
Elliott, K.H., Betini, G.S., Norris, D.R., 2017. Fear creates an allee effect: experimental evidence from seasonal populations. Proc. R. Soc. Lond. B 284, 20170878.
Fontaine, J.J., Martin, T.E., 2006. Parent birds assess nest predation risk and adjust their reproductive strategies. Ecol. Lett. 9 (4), 428–434.
Freedman, H.I., Wolkowicz, G.S.K., 1986. Predator-prey systems with group defence: the paradox of enrichment revisited. Bull. Math. Biol. 48 (5-6), 493–508.
Gard, T., Hallam, T., 1979. Persistence in food Webs-Lotka-Volterra food chains. Bull. Math. Biol. 41 (6), 877–891.
Ghalambor, C.K., Peluc, S.I., Martin, T.E., 2013. Plasticity of parental care under the risk of predation: how much should parents reduce care? Biol. Lett. 9 (4), 20130154.
Guckenheimer, J., Holmes, P.J., 1983. Nonlinear Oscillations, Dynamical Systems and Bifurcation of Vector Fields. Springer, New York.
Hassard, B.D., Kazarinoff, Y.H., Wan, Y.H., 1981. Theory and Applications of Hopf bifurcation. Cambridge University Press, Cambridge.
Holling, C.S., 1959a. The components of predation as revealed by a study of small-mammal predation of the european pine sawfly. Can. Entomol. 91 (5), 293–320.
Holling, C.S., 1959b. Some characteristics of simple types of predation and parasitism. Can. Entomol. 91 (7), 385–398.
Holling, C.S., 1965. The functional response of predators to prey density and its role in mimicry and population regulation. Mem. Entomol. Soc. Can.Suppl. S45, 5–60.
Hua, F., Sieving, K.E., Fletcher, R.J., Wright, C.A., 2014. Increased perception of predation risk to adults and offspring alters avian reproductive strategy and performance. Behav. Ecol. 25 (3), 509–519.
Khajanchi, S., 2014. Dynamic behavior of a Beddington-Deangelis type stage structured predator-prey model. Appl. Math. Comput. 244, 344–360.
Khajanchi, S., 2017a. Modeling the dynamic of stage-structure predator-prey system with Monod-Haldane type response function. Appl. Math. Comput. 302, 122–143.
Khajanchi, S., 2017b. Uniform persistence and global stability for a brain tumor and immune system interaction. Biophys. Rev. Lett. 12 (04), 187–208.
Khajanchi, S., Banerjee, S., 2017. Role of constant prey refuge on stage structure predator-prey model with ratio dependent functional response. Appl. Math. Comput. 314, 193–198.
Krivan, V., 2007. The lotka-volterra predator-prey model with foraging predation risk trade-offs. Am Nat. 170, 1–782.
Kuang, Y., Freedman, H.I., 1988. Uniqueness of limit cycles in Gause-type models of predator-prey systems. Math. Biosci. 88 (1), 67–84.
Lima, S., Dill, L.M., 1990. Behavioral decisions made under the risk of predation: a review and prospectus. Can. J. Zool. 68, 619–640.
May, R.M., 1972. Limit cycles in predator-prey communities. Science 177 (4052), 900–902.
Mondal, S., Maiti, A., Samanta, G.P., 2018. Effects of fear and additional food in a delayed predator-prey model. Biophys. Rev. Lett. 13 (04), 157–177.
Preisser, E.L., Bolnick, D.I., 2008. The many faces of fear: comparing the pathways and impacts of non-consumptive predator effects on prey populations. PloS ONE 3, e2465.
Ruan, S., Xiao, D., 2001. Global analysis in a predator-prey system with nonmonotonic functional response. SIAM J. Appl. Math. 61, 1445–1472.
Ryu, K., Ko, W., Haque, M., 2018. Bifurcation analysis in a predator-prey system with a functional response increasing in both predator and prey densities. Nonlinear Dyn. 94 (3), 1639–1656.
Sheriff, M.J., Krebs, C.J., Boonstra, R., 2009. The sensitive hare: sublethal effects of predator stress on reproduction in snowshoe hares. J. Anim. Ecol. 78 (6), 1249–1258.
Sugie, J., Kohno, R., Miyazaki, R., 1997. On a predator-prey system of holling type. Proc. Am. Math. Soc. 125 (7), 2041–2050.
Takeuchi, Y., Wang, W., Nakaoka, S., Iwami, S., 2009. Dynamical adaptation of parental care. Bull. Math. Biol. 71, 931–951.
Wang, J., Cai, Y., Fu, S., Wang, W., 2019. The effect of the fear factor on the dynamics of a predator-prey model incorporating the prey refuge. Chaos 29, 83109.
Wang, X., Zanette, L., Zou, X., 2016. Modelling the fear effect in predator-prey interactions. J. Math. Biol. 75 (5), 1179–1204.
Wang, X., Zou, X., 2017. Modeling the fear effect in predator-prey interactions with adaptive avoidance of predators. Bull. Math. Biol. 79, 13–25.
Wirsing, A.J., Ripple, W.J., 2011. A comparison of shark and wolf research reveals similar behavioural responses by prey. Front. Ecol. Environ. 9 (6), 335–341.
Zanette, L.Y., White, A.F., Allen, M.C., Clinchy, M., 2011. Perceived predation risk reduces the number of offspring songbirds produce per year. Science 334 (6061), 1398–1401.
Zhanga, H., Cai, Y., Fu, S., Wan, W., 2019. Impact of the fear effect in a prey-predator model incorporating a prey refuge. Appl. Math. Comput. 356, 328–337.